

# Typical Algorithms for Estimating Hurst Exponent: A Data Analyst's Perspective

Hong-Yan Zhang<sup>†\*</sup>, Zhi-Qiang Feng<sup>†</sup>, Si-Yu Feng<sup>‡</sup> and Yu Zhou<sup>†</sup>

<sup>†</sup> *School of Information Science and Technology, Hainan Normal University, Haikou 571158, China*

<sup>‡</sup> *School of Geography, University of Leeds, LS2 9JT, United Kingdom*

October 21, 2024

## Abstract

The Hurst exponent is a significant indicator for characterizing the time sequence (TS) with the long-term memory property. It has wide applications in physics, technologies, engineering, mathematics, statistics, economics, psychology and so on. Currently, the available methods for estimating the Hurst exponent of time sequence with long-term memory can be divided into different categories: time-domain methods and spectrum-domain methods based on the representation of time sequence, linear regression methods and Bayesian methods based on parameter estimation methods. Although various methods are discussed in literature, there are still some deficiencies: the descriptions of the estimation methods are just mathematics-oriented and the algorithmic pseudo-codes are missing; the effectiveness and accuracy of the estimation algorithms are not clear; the classification of estimation methods is not considered and the lack of guidance for selecting the estimation methods decreases the efficiency of data analysis. The contributions of this article lie in four folds: the optimal sequence partition method is proposed for designing the estimation algorithms for Hurst exponent; the mathematical computational methods for estimating the Hurst exponent are converted to algorithmic pseudo-codes in the sense of computer science, which improves the understandability and usability of the estimation methods and also reduces the difficulty of implementation these methods with concrete computer programming languages; the performance assessment is carried for the typical estimation algorithms via the ideal time sequences with given Hurst exponent and the practical data of TS; the guidance for selecting the algorithms for estimating the Hurst exponent is presented. It is expected that the assessment of the various estimation methods could help the researchers to select, implement and apply the estimation algorithms of interest in practical situations in an easy way.

**Keywords:** Time sequence (TS); Hurst exponent; Sequence partition; Algorithmic pseudo-code; Understandability and usability; Performance assessment

## Contents

<b>1</b>	<b>Introduction</b>	<b>3</b>
<b>2</b>	<b>Preliminaries</b>	<b>5</b>
2.1	Hurst Exponent . . . . .	5
2.2	Integers and Division . . . . .	8
2.3	Discrete Fourier Transform . . . . .	8
2.4	Discrete Wavelet Transform . . . . .	9
2.5	Fractional Gaussian Noise . . . . .	9
2.6	Linear Regression and Parameters Estimation . . . . .	10
2.7	Algorithm for Solving Fixed-Point in Euclidean Space . . . . .	12
2.8	Algorithm for Searching a Local Minimum of Single-variable Function . . . . .	12

---

\*Correspondence author, email: hongyan@hainnu.edu.cn

<b>3</b>	<b>Optimal Sequence Partition</b>	<b>13</b>
3.1	Fundamental Operations on Time Sequences . . . . .	13
3.1.1	Cumulative Sum of Sequence . . . . .	13
3.1.2	Sequence Partition . . . . .	13
3.2	Steps and Algorithms for Optimal Sequence Partition . . . . .	14
3.2.1	Steps for Optimal Sequence Partition . . . . .	14
3.2.2	Brute-force Searching Method for Specifying Bounded Proper Factors of Composite Integer . . . . .	14
3.2.3	Searching Optimal Approximate Length of Sequence . . . . .	14
3.2.4	Specifying the Parameters of Subsequence . . . . .	15
<b>4</b>	<b>Typical Methods For Estimating Hurst Exponent</b>	<b>15</b>
4.1	Central Estimation . . . . .	16
4.1.1	Principle of Central Estimator . . . . .	16
4.1.2	Algorithm for Central Estimator . . . . .	16
4.2	Generalized Hurst Exponent Method (GHE) . . . . .	17
4.2.1	Principle of GHE Estimator . . . . .	17
4.2.2	Algorithm for GHE Estimator . . . . .	18
4.3	Higuchi Method (HM) . . . . .	18
4.3.1	Principle of Higuchi Estimator . . . . .	18
4.3.2	Algorithm for Higuchi Estimator . . . . .	19
4.4	Detrended Fluctuation Analysis (DFA) . . . . .	19
4.4.1	Principle of DFA Estimator . . . . .	19
4.4.2	Algorithm for DFA Estimator . . . . .	22
4.5	Rescaled Range Analysis (R/S Analysis) . . . . .	23
4.5.1	Principle of R/S Estimator . . . . .	23
4.5.2	Algorithm for R/S Estimator . . . . .	25
4.6	Triangles Total Areas (TTA) Method . . . . .	25
4.6.1	Principle of TTA Estimator . . . . .	25
4.6.2	Algorithm for TTA Estimator . . . . .	26
4.7	Periodogram Method (PM) . . . . .	27
4.7.1	Principle of Periodogram Estimator . . . . .	27
4.7.2	Algorithm for Periodogram Estimator . . . . .	28
4.8	Discrete Wavelet Transform (DWT) Method . . . . .	28
4.8.1	Average Wavelet Coefficient Method (AWC) . . . . .	28
4.8.2	Variance Versus Level (VVL) Method . . . . .	29
4.8.3	Algorithm for DWT Estimator . . . . .	29
4.9	Local Whittle (LW) Method . . . . .	30
4.9.1	Principle of LW Estimator . . . . .	30
4.9.2	Algorithm for LW Estimator . . . . .	30
4.10	Least Squares via Standard Deviation (LSSD) . . . . .	31
4.10.1	Principle of LSSD Estimator . . . . .	31
4.10.2	Algorithm for LSSD Estimator . . . . .	32
4.11	Least Squares via Variance (LSV) . . . . .	34
4.11.1	Principle of LSV Estimator . . . . .	34
4.11.2	Algorithm for LSV Estimator . . . . .	34
<b>5</b>	<b>Performance Assessment for the Typical Algorithms</b>	<b>36</b>
5.1	Experimental Setup . . . . .	36
5.2	Random Sequence and Hurst Exponent . . . . .	36
5.3	Estimation with Fractional Gaussian Noise Sequence . . . . .	36
5.4	Relative Error of Estimating Hurst Exponent . . . . .	38
5.5	Impacts of Norm and Optimization Method on Estimation Performance . . . . .	38
5.6	Hurst Exponent of Reaction Time Sequence . . . . .	39

# 1 Introduction

The *long-term memory* (LTM) of *time sequence* (TS) was discovered in 1951 by Harold E. Hurst [1,2]. The LTM is also named with the *long range dependence* (LRD). The LTM exists in a wide range of natural phenomena, such as rainfall, tree rings, solar flares and so on [3]. In order to qualitatively explore the the changes of river water level, Hurst proposed the exponent, denoted by  $H$  and named with *Hurst exponent* or *Hurst index* for his contribution, to characterize the *time sequence with long-term memory* (TS-LTM).

It is a fundamental problem to estimate the Hurst exponent for the time sequence with LTM. In the past decades, researchers developed various methods for estimating the Hurst exponent. **Figure 1** illustrates 13 typical methods and technical framework for estimating the Hurst exponent of TS-LTM. The estimation methods can be classified with different categories based on two criteria:

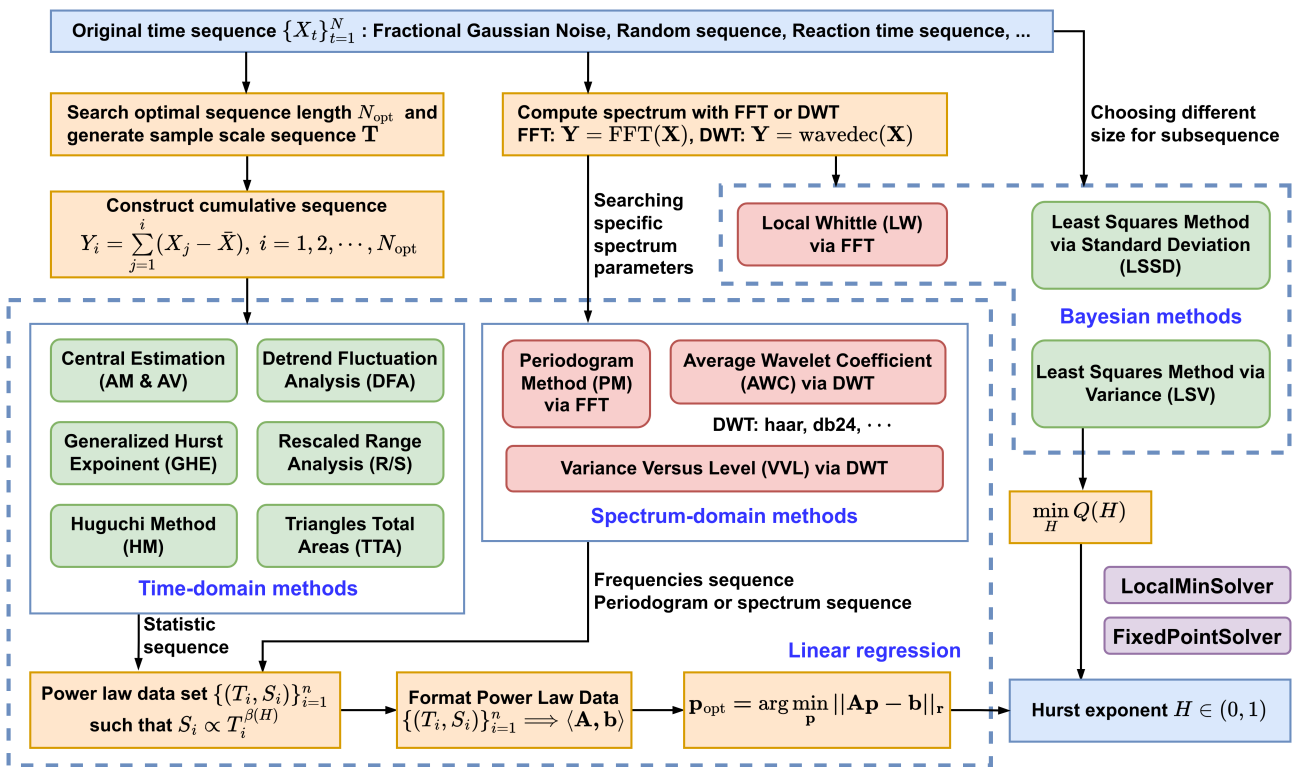


Figure 1: Typical Algorithms and Technical Framework for Estimating Hurst Exponent of TS-LTM

- ① time-domain methods and spectrum-domain methods based on the representation of TS;
- ② linear regression methods and Bayesian methods based on the parameter estimation method.

As listed in **Table 1**, there are four types of estimation methods according to the representation ways of TS and the parameter estimation techniques for the Hurst exponent. We now give a brief introduction to the history and ideas behind them.

The time-domain estimation method has attracted lots of researchers for several decades. For instance, Beran [4] constructed the *aggregate variance* (AV) method for estimating the Hurst exponent using the sample variance in 1994. After that, Taqqu [5] proposed the *absolute moments* (AM) method

Table 1: Classification of 13 typical estimation methods

METHOD	PARAMETER ESTIMATION	
	Linear Regression	Bayesian
SEQUENCE REPRESENTATION		
Time-domain	AM, AV, GHE, HM, R/S, DFA, TTA	LSSD, LSV
Spectrum-domain	PM, AWC, VVL	LW

in 1995. The AV method and AM method are unified as the *central estimation*. In 1991, Barabási [6] proposed the *generalized Hurst exponent* (GHE) method via the  $q$ -th order moments for estimating the Hurst exponent, which is similar to the central estimation. In 1988, the *Higuchi method* [7] was constructed to calculate the fractal dimension of a time sequence. Due to the constant offset between the fractal dimension and the Hurst exponent, this method can be applied to estimate the Hurst exponent of a time sequence. In 1994, Peng et al. [8] proposed the *detrended fluctuation analysis* (DFA) method which was also called *residuals of regression* method [5]. The DFA method was initially utilized to analyze whether non-coding regions in DNA sequences have long-range correlations, and the resulting value is the Hurst exponent. Inspired by the DFA method, Lotfalinezhad et al. [9] and proposed the *triangles total areas* (TTA) method in 2020 to estimate the Hurst exponent via triangles total areas. Subsequently, Gómez et al. [10] an effective theoretical framework for the TTA method and a slightly different method called *triangle area* (TA) method in 2021. In addition to these conventional time-domain methods, Tyrallis [11] and Koutsoyiannis [12] have proposed two Bayesian statistics estimation methods — *least squares via standard deviation* (LSSD) and *least squares via variance* (LSV) — based on serial variance and standard deviation in 2003 respectively. In 2023, Likens [13] compared the performances of these two Bayesian methods and the DFA method and declared that the Bayesian methods are better than the DFA method, especially when the length of the TS is short.

The spectrum-domain estimators have been studied since the beginning of the era of 1980s. For example, Hosking et al. [14] discovered that certain time sequences have similar spectral density features in the low-frequency range in 1981. Subsequently, this property was used by Geweke and Porter-Hudak [15] to propose the *periodogram* (PM) method for estimating the Hurst exponent. Moreover, this property was also used by Künsch [16] and Robinson [17] to develop the *local whittle* (LW) method which is also named *Gaussian semi-parametric estimation*. Phillip systematically assessed these two spectrum-domain methods in 2004 [18]. In 1989, Flandrin [19] discovered the relation of wavelet transform to fractional Brownian motion. In 1992, Flandrin found [20] the relationship between the variance of wavelet coefficients and the Hurst exponent based on the discrete wavelet transform. In 1998, Ingve Simonsen et al. [21] proposed the *average wavelet coefficient method* (AWC) for estimating the Hurst exponent using the DWT, and then applied this method to measure the anti-correlation in the Nordic electricity spot market in 2003 [22].

In recent years, the emphasis of the researchers are focused on the applications of Hurst exponent and performance evaluation of the estimation methods. We now give some examples here. Zhang et al. [23] in 2017 analyzed the reaction time data and Li et al. [24] in 2018 studied the features clustering problem with the R/S analysis. Moundjian et al. [25] applied the DFA method to calculate the fractal statistical properties of the gait time-series to quantify gait dynamics by the outcome measure alpha in 2020. Shang [26] in 2020 compared the limited sample variance, variance and mean square deviation of some Hurst exponent estimators in time and spectrum domain with the ARFIMA model. Hamza et al. [27] in 2021 proposed the *mean absolute scaled error* (MASE) index of different Hurst exponent estimators based on the *Fractional Brownian motion* (FBM). Lahmiri [28] in 2023 used the GHE method to estimate the Hurst exponent of electrocardiogram data, providing auxiliary features for the classification of heart disease data. Recently, Paul et al. [29] in 2024 has taken the Hurst exponent

to measure and compare the statistical properties of fracture profiles under various micro-structural conditions, correlating these characteristics with the fracture mechanisms of the material.

Although various methods are discussed in literature, there are still some deficiencies from the perspective of data analysts:

- the descriptions of the estimation methods are just mathematics-oriented and the general algorithmic pseudo-codes are missing;
- the effectiveness and accuracy of the estimation algorithms are not clear;
- the classification of estimation methods is not considered;
- the technical framework for estimating the Hurst exponent is missing; and
- a lack of guidance for selecting the estimation methods decreases the efficiency of data analysis.

Motivated by the understandability of the estimation principle and the usability of estimation algorithms for the Hurst exponent arising in data analysis, our contributions of this work lie in the following aspects:

- 1) the optimal sequence partition method is proposed for designing the estimation algorithms for Hurst exponent;
- 2) the mathematical computational methods for estimating the Hurst exponent are converted to algorithmic pseudo-codes in the sense of computer science, which improves the understandability and usability of the estimation methods and also reduces the difficulty of implementation these methods with concrete high-level computer programming languages such as C/C++, Octave/MATLAB, SciLab, Python, Julia, R, Java, Rust and so on;
- 3) the performance assessment is carried for the typical estimation algorithms via the ideal time sequences with given Hurst exponent and the practical data of TS-LTM;
- 4) guidance for selecting the algorithms for estimating the Hurst exponent is presented based on the performance evaluation.

The contents of this paper are organized as follows: Section 2 provides the preliminaries for the data analysts; Section 3 deals with the optimal sequence partition; Section 4 copes with the typical methods for estimating the Hurst exponent; Section 5 is devoted to the performance assessment for the typical algorithms; and Section 6 summarizes the conclusions. For the convenience of reading for the readers, the abbreviations used in this paper has been summarized in **Table 2**.

## 2 Preliminaries

### 2.1 Hurst Exponent

Mathematically, a time sequence is just a stochastic process with a discrete parameter “time”, which can be denoted by  $X : \Omega \times \mathbb{Z} \rightarrow \mathbb{R}$ ,  $(\omega, t) \mapsto x$  or simply by

$$x = X(\omega, t) = X_t(\omega) \quad (1)$$

where the  $\Omega$  is the sample space of a probability space  $(\Omega, \mathcal{F}, \Pr)$  and the  $\omega \in \Omega$  in (1) is a sample point. The mapping  $X(\omega, t) = X_t(\omega)$  in (1) could be denoted by  $X_t$  by omitting the variable  $\omega \in \Omega$  according to the custom of data analysis and signals processing. The Hurst exponent is closely related to the stationary TS-LTM [4]:

**Definition 1.** *Let  $X_t$  be a stationary stochastic process and  $k \in \mathbb{N}$  be the time lagging parameter,  $\rho(k)$  is the autocorrelation function of  $X_t$ . If there exists a real number  $\alpha \in (0, 1)$  and a constant  $c_\rho > 0$  such that asymptotically  $\rho(k) \sim c_\rho k^\alpha$  for  $k \rightarrow \infty$ , viz.*

$$\lim_{k \rightarrow \infty} \frac{\rho(k)}{c_\rho k^{-\alpha}} = 1, \quad (2)$$

*then  $X_t$  is called a stationary process with long-term memory.*

Table 2: Nomenclatures

No.	Abbreviation	Interpretation
1	TS	Time Sequence
2	LTM, LRD	Long-Term Memory, also named with the Long Range Dependence
3	SRD	Short Range Dependence
4	TS-LTM	Time Sequence with Long-Term Memory
5	FGN	Fractional Gaussian Noise, which is used as sample sequence for verification and validation
6	MASE	Mean Absolute Scaled Error
7	FBM	Fractional Brownian Motion
8	DFT, IDFT	Discrete Fourier Transform, Inverse Discrete Fourier Transform
9	FFT	Fast Fourier Transform
10	DWT	Discrete Wavelet Transform
11	LS	Least Squares
12	HS	Human-Speaker
13	TTS	Text-To-Speech
14	RT	Reaction Time
15	MLE	Maximum Likelihood Estimation
16	KS	Kolmogrov-Smirnov
M01	AM	Absolute Moments, where the first order central moment is used in Central estimation
M02	AV	Aggregate Variances, where the second order central moment is used in Central estimation
M03	GHE	Generalized Hurst Exponent $H(q)$ , where $q$ is the order
M04	HM	Higuchi method, which was constructed by Higuchi in 1988
M05	DFA	Detrended Fluctuation Analysis, which used the residual of regression
M06	R/S	Rescaled Range Analysis, where $R = \max_t X_t - \min_t X_t$ and $S = \text{Std}(X_t)$ for the TS $\{X_t\}_{t=1}^N$
M07	TTA	Triangles Total Areas
M08	PM	Periodogram Method
M09	AWC	Average Wavelet Coefficient
M10	VVL	Variance Versus Level
M11	LW	Local Whittle, also named Gauss semi-parametric estimation
M12	LSSD	Least Squares via Standard Deviation
M13	LSV	Least Squares via Variance

There are various jargons for the LTM of a stationary process such as *long-range dependence*, *strong dependence*, *slowly decaying* and *long-range correlations*. The LTM is the counterpart of *short range dependency* (SRD). The autocorrelation function of a time sequence with short-range dependency exponentially decay to zero when the time lag increases. In contrast, the autocorrelation function of a time sequence with long-term memory decays moderately, following a power-law decay pattern as described by (2).

The Hurst exponent  $H$  is a measure of the long-term memory capability of a time sequence. Usually, the range of  $H$  is the open interval  $(0, 1)$  [4]. A value of  $H \in (0.5, 1)$  indicates the LTM or LRD while  $H \in (0, 0.5)$  indicates the SRD, and  $H = 0.5$  represents a random sequence in which observations are completely uncorrelated. The essence of the Hurst exponent is to reflect how the range of fluctuation in a TS changes with the time span.

Let  $E\{\cdot\}$  be the expectation operator and  $\mathcal{A}_t^{k:m}\{\cdot\}$  be the arithmetic average operator defined by

$$\mathcal{A}_t^{k:m}\{X_{\alpha t + \beta s}\} = \frac{1}{m - k + 1} \sum_{t=k}^m X_{\alpha t + \beta s} \quad (3)$$

where the  $t$  in (3) denotes the variable for summation,  $k$  and  $m$  denote the range of  $t$ . Particularly, for  $(\alpha, \beta, m, k) = (1, 0, 1, n)$ , the notation for the arithmetic average can be simplified by

$$\bar{X} = \mathcal{A}(X_t) = \mathcal{A}_t^{1:n}\{X_t\} = \frac{1}{n} \sum_{t=1}^n X_t. \quad (4)$$

Let  $\mathcal{S}_t^{1:n}\{\cdot\}$  be the standard deviation operator, we have

$$\mathcal{S}_t^{1:n}\{X_t\} = \sqrt{\frac{1}{n-1} \sum_{t=1}^n (X_t - \mathcal{A}(X_t))^2} \quad (5)$$

Equations (4) and (5) are fundamental for statistics computing for time sequences. For the  $n$  consecutive samples  $\{X_t\}_{t=1}^n$ , the range and standard deviation are specified by

$$R(n) = \max_{1 \leq t \leq n} X_t - \min_{1 \leq t \leq n} X_t \quad (6)$$

and

$$S(n) = \mathcal{S}_t^{1:n}\{X_t\} \quad (7)$$

respectively. The R/S statistic is defined by the ratio of  $R(n)$  in (6) to  $S(n)$  in (7), viz.

$$\mathcal{R}_X(n) = \frac{R(n)}{S(n)}. \quad (8)$$

Historically, it was Hurst who discovered that there exists a constant  $H$  such that the  $\mathcal{R}_X(n)$  in (8) is dominated by the power  $n^H$  asymptotically. It is a fundamental problem that how to estimate the Hurst exponent of TS robustly, precisely and efficiently. Currently, there are various methods for estimating the Hurst exponent. According to the equivalent representation domain for the time sequence, there are two fundamental categories for the available estimation methods:

- time-domain method, in which the TS  $\{X_t : 1 \leq t \leq N\}$  is used directly and the Hurst exponent is estimated by revealing the characteristics of some statistical properties change with the variation of observation period.
- spectrum-domain method, in which the *discrete Fourier transform* (DFT) and *discrete wavelet transform* (DWT) are taken for the time sequence  $\{X_t : 1 \leq t \leq N\}$ .

Mathematically, Hurst's observation can be expressed by

$$E\{\mathcal{R}_X(n)\} \sim n^H \quad (9)$$

asymptotically for sufficiently large  $n$ , in which  $E$  is the operator of expectation in the sense of probability and mathematical statistics. The method of estimating the Hurst exponent  $H$  according to (9) is called the *R/S analysis* or *range rescaled analysis* since  $R(n)/S(n)$  means rescaling the range  $R(n)$  with the standard deviation  $S(n)$ . The R/S analysis was popularized by Mandelbrot with his great work on the theory of fractal [30–32] and it was the first kind of time-domain method. An important result obtained by Mandelbrot is the relation of fractal dimension  $D$  and the Hurst exponent  $H$ , which can be expressed by

$$D + H = 2. \quad (10)$$

Equation (10) is important for the Higuchi algorithm for estimating the Hurst index  $H$ .

## 2.2 Integers and Division

For the positive integers  $a, b \in \mathbb{N}$  and  $b \geq 2$ , we can find a non-negative integer  $q \in \mathbb{Z}^+$  such that

$$a = bq + r, \quad 0 \leq r \leq b - 1 \quad (11)$$

If  $r = 0$ , then  $b$  divides  $a$  and  $b$  is a factor of  $a$ , which can be denoted by  $b \mid a$ . If  $r \neq 0$ , then we denote it as  $b \nmid a$ . For  $a \geq 2$ , if  $b \mid a$  implies that  $b$  must be 1 or  $a$ , then  $a$  is called a *prime number*, otherwise it is called a *composite number*. The factor  $b$  of the composite number  $a$  such that  $b \notin \{1, a\}$  is called a *proper factor*.

The integer  $q$  in (11) can be calculated by  $q = \lfloor \frac{a}{b} \rfloor$  where  $\lfloor x \rfloor$  denotes the lower integer of  $x$  such that  $\lfloor x \rfloor \leq x < \lfloor x \rfloor + 1$ . Similarly, the  $\lceil x \rceil$  denotes the upper integer of  $x$  such that  $x \leq \lceil x \rceil < x + 1$ . For illustration, we have  $\lfloor \pi \rfloor = 3$ ,  $\lfloor -\pi \rfloor = -4$ ,  $\lceil \pi \rceil = 4$  and  $\lceil -\pi \rceil = -3$ .

The set of proper factors of the composite number  $a \in \mathbb{N}$  can be denoted by

$$S_{\text{pf}}(a) = \{d \in \mathbb{N} : d \mid a, d \geq 2, d \neq a\}.$$

Let  $a$  be composite number and  $w \in \{2, \dots, \lfloor \sqrt{a} \rfloor\}$  be a integer for lower bound, then

$$S_{\text{bpf}}(a, w) = \left\{ d \in S_{\text{pf}}(a) : w \leq d \leq \left\lfloor \frac{a}{w} \right\rfloor \right\} \quad (12)$$

is called the set of *bounded proper factors* of  $a$ . The cardinality of the set  $S_{\text{bpf}}(a, w)$  is denoted by  $|S_{\text{bpf}}(a, w)|$ , which means the number of the elements in the set. For example, we have  $\lfloor \sqrt{48} \rfloor = 6$  and  $S_{\text{pf}}(48) = \{2, 3, 4, 6, 8, 12, 24\}$ . Thus for  $w \in \{2, 3, 4, 5, 6\}$ , equation (12) implies that

$$\left\{ \begin{array}{ll} S_{\text{bpf}}(48, 2) = \{2, 3, 4, 6, 8, 12, 16, 24\}, & |S_{\text{bpf}}(48, 2)| = 8; \\ S_{\text{bpf}}(48, 3) = \{3, 4, 6, 8, 12, 16\}, & |S_{\text{bpf}}(48, 3)| = 6; \\ S_{\text{bpf}}(48, 4) = \{4, 6, 8, 12\}, & |S_{\text{bpf}}(48, 4)| = 4; \\ S_{\text{bpf}}(48, 5) = \{6, 8\}, & |S_{\text{bpf}}(48, 5)| = 2; \\ S_{\text{bpf}}(48, 6) = \{6, 8\}, & |S_{\text{bpf}}(48, 6)| = 2. \end{array} \right.$$

## 2.3 Discrete Fourier Transform

For the discrete TS  $\{X_1, \dots, X_N\}$  with length  $N$ , its DFT is defined by [33]

$$\hat{X}_k = \sum_{t=1}^N X_t e^{-\frac{2\pi i}{N}(k-1)(t-1)}, \quad 1 \leq k \leq N \quad (13)$$

where  $i = \sqrt{-1}$ . The sequence  $\{\hat{X}_k : 1 \leq k \leq N\}$  is called the frequency spectrum of  $\{X_t : 1 \leq t \leq N\}$ . The *inverse discrete Fourier transform* (IDFT) for (13) is defined by

$$X_t = \frac{1}{N} \sum_{k=1}^N \hat{X}_k e^{+\frac{2\pi i}{N}(k-1)(t-1)}, \quad 1 \leq t \leq N \quad (14)$$

Usually the DFT is implemented with the *fast Fourier transform* (FFT) proposed by Cooley and Tukey in 1965 [34] in order to reduce the computational complexity from  $\mathcal{O}(N^2)$  to  $\mathcal{O}(N \log_2 N)$ . The equation (14) is significant for the spectrum methods for estimating the Hurst exponent and generating the FGN.

## 2.4 Discrete Wavelet Transform

A *discrete wavelet transform* (DWT) is a wavelet transform that decomposes the host signal into wavelets that are discontinuous. Its temporal resolution makes it more attractive over DFT since it contains more information carried both in time and frequency [35].

For the length  $N$  of the TS  $\{X_t : 1 \leq t \leq N\}$ , we can set the scaling parameter

$$a \in \{1, 2^1, 2^2, \dots, 2^{J-1}\}, \quad J = \lceil \log_2 N \rceil \quad (15)$$

and position parameter

$$b \in I_a = \{0, 1, 2, \dots, a-1\} \quad (16)$$

respectively. With the help of (15) and (16), the scaling functions  $\varphi_{a,b}(t)$  and wavelet functions  $\psi_{a,b}(t)$  are defined by

$$\begin{cases} \varphi_{a,b}(t) = \sqrt{a} \cdot \varphi(a(t-1) - b), \\ \psi_{a,b}(t) = \sqrt{a} \cdot \psi(a(t-1) - b), \end{cases} \quad 1 \leq t \leq N \quad (17)$$

Then the DWT of the discrete time signal  $\{X_t : 1 \leq t \leq N\}$  is defined with the scale coefficients  $W_{\mathbf{X}}^\varphi(a, b)$  and detail coefficients  $W_{\mathbf{X}}^\psi(a, b)$ , viz. [36]:

$$\begin{cases} W_{\mathbf{X}}^\varphi(a, b) = \frac{1}{\sqrt{N}} \sum_{t=1}^N \varphi_{a,b}(t) X_t, \\ W_{\mathbf{X}}^\psi(a, b) = \frac{1}{\sqrt{N}} \sum_{t=1}^N \psi_{a,b}(t) X_t. \end{cases} \quad (18)$$

Once the  $\varphi_{a,b}(t)$  and  $\psi_{a,b}(t)$  are computed by (17), the  $W_{\mathbf{X}}^\varphi(a, b)$  and  $W_{\mathbf{X}}^\psi(a, b)$  can be obtained according to (18). In this paper, only the detail coefficients of the DWT is concerned and we set

$$\text{DWT}_b^a(\mathbf{X}, \psi) = W_{\mathbf{X}}^\psi(a, b). \quad (19)$$

Note that the choice of the wavelet function  $\psi(t)$  in (19) is not unique for the continuous and discrete wavelet transforms. Both the Harr wavelet [37] and Daubechies wavelet [38] are satisfactory for estimating the Hurst exponent of the time sequences.

## 2.5 Fractional Gaussian Noise

The *fractional Gaussian noise* (FGN), which is closely associated with the FBM [39], is a special type of time sequences with the self-similarity characterized by its autocorrelation. The autocorrelation function of the FGN sequence  $U = \{u_n : n = 0, 1, 2, \dots\}$  is [40]

$$\phi_U(\tau) = \text{E}\{u_n u_{n+\tau}\} = \frac{1}{2}(|\tau+1|^{2H} - 2|\tau|^{2H} + |\tau-1|^{2H}) = \phi_U(-\tau) \quad (20)$$

where  $\tau \in \mathbb{Z}^+$  is the time lag. With the help of Newton's binomial theorem, we can deduce that

$$(1 \pm \tau^{-1})^{2H} = 1 \pm \binom{2H}{1} \cdot \tau^{-1} + H(2H-1)(\pm\tau^{-1})^2 + \mathcal{O}(\tau^{-3}) \quad (21)$$

for sufficiently large  $\tau$ . Substitute (21) into (20), the autocorrelation function can be expressed by

$$\phi_U(\tau) = \frac{\tau^{2H}}{2} [(1 + \tau^{-1})^{2H} - 2 + (1 - \tau^{-1})^{2H}] = H(2H-1)\tau^{2H-2} + \mathcal{O}(\tau^{-3}). \quad (22)$$

Equation (22) shows that we have the asymptotic property

$$\phi_U(\tau) \propto H(2H-1)\tau^{2H-2} \iff \ln \phi_U(\tau) \sim \alpha_{\text{fgn}} + \beta_{\text{fgn}} \ln \tau \quad (23)$$

for the sufficiently large time lag  $\tau$  and for the constants  $\alpha_{\text{fgn}}$  and  $\beta_{\text{fgn}} = 2H - 2$ .

Theoretically, the FGN sequence is of self-similarity strictly. The property specified by (23) can be utilized to generate the FGN sequences with given Hurst exponent [41]. The procedure GENTIMESEQFGN described in **Algorithm 1** is of great significance for the verification and validation of the estimation algorithms for the Hurst exponent.

---

**Algorithm 1** Generating the FGN sequence as the ideal time sequence with specified  $H$ .

---

**Input:** Sequence length  $\ell$ , hurst exponent  $H$ .

**Output:** The FGN sequence  $U = \{u_t : 0 \leq t \leq \ell\}$ .

```

1: procedure GENTIMESEQFGN( $\ell, H$ )
2:    $\boldsymbol{\rho} \leftarrow \mathbf{0} \in \mathbb{R}^{1 \times \ell}$ ; // For the autocorrelation function
3:   for  $k \in \langle 0, 1, \dots, \ell - 1 \rangle$  do
4:      $\rho_{k+1} \leftarrow 0.5 \cdot (|k-1|^{2H} - 2|k|^{2H} + |k+1|^{2H})$ ;
5:   end for
6:    $\mathbf{g} \leftarrow \text{FFT}([\boldsymbol{\rho}(1:\ell), 0, \boldsymbol{\rho}(\ell:2)])$ ; // FFT for (13)
7:    $\mathbf{V} = \sqrt{\mathbf{g}}$ ; // Eigenvalues of the correlation sequence
8:    $\mathbf{m} \leftarrow \mathbf{0} \in \mathbb{R}^{1 \times \ell}$ ,  $\mathbf{n} \leftarrow \mathbf{0} \in \mathbb{R}^{1 \times \ell}$ ;
9:    $\mu \leftarrow 0, \sigma \leftarrow 1$ ; // for  $\mathcal{N}(0, 1)$ 
10:   $\mathbf{m} \leftarrow \text{GENTIMESEQGAUSS}(\mu, \sigma, \ell)$ ;
11:   $\mathbf{n} \leftarrow \text{GENTIMESEQGAUSS}(\mu, \sigma, \ell)$ ;
12:   $\mathbf{w} \leftarrow \mathbf{0} \in \mathbb{R}^{1 \times 2\ell}$ ;
13:   $w_1 \leftarrow \frac{V_1}{\sqrt{2\ell}} \cdot m_1$ ;
14:  for  $j \in \langle 2, 3, \dots, \ell \rangle$  do
15:     $w_j \leftarrow \frac{V_j}{\sqrt{4\ell}} \cdot (m_j + i \cdot n_j)$ ; //  $i = \sqrt{-1}$ 
16:     $w_{\ell+j} \leftarrow \frac{V_{\ell+j}}{\sqrt{4\ell}} \cdot (m_{\ell-j+2} - i \cdot n_{\ell-j+2})$ ;
17:  end for
18:   $w_{\ell+1} \leftarrow \frac{V_{\ell+1}}{\sqrt{2\ell}} \cdot n_1$ ;
19:   $\mathbf{f} \leftarrow \Re(\text{FFT}(\mathbf{w}))$ ; // taking the real part
20:   $U \leftarrow \ell^{-H} \mathbf{f}(1:j)$ ;
21:  return  $U$ ;
22: end procedure

```

---

Note that for the  $d$ -dimensional vector  $\mathbf{v} \in \mathbb{R}^{d \times 1}$  or  $\mathbf{v} \in \mathbb{R}^{1 \times d}$ , the notation  $\mathbf{v}(i:r)$  means taking the sub-vector of  $\mathbf{v}$ , namely

$$\mathbf{v}(i:r) = \begin{cases} (v_i, v_{i+1}, \dots, v_{r-1}, v_r), & i < r; \\ (v_i, v_{i-1}, \dots, v_{r+1}, v_r), & i > r. \end{cases} \quad (24)$$

Equation (24) is significant in matrix computation and it will be encountered for many times in this paper. Furthermore, the procedure GENTIMESEQGAUSS( $\mu, \sigma, \ell$ ) is used to generate the time sequence with normal distribution in which  $\mu$  is the expectation,  $\sigma$  is the standard deviation and  $\ell$  is the length of the sequence. Note that the sequences  $\mathbf{m}$  and  $\mathbf{n}$  should be generated independently.

## 2.6 Linear Regression and Parameters Estimation

The estimation of Hurst exponent is built on the method of linear regression for parameter estimation. Suppose the asymptotic behavior of data set  $\{(x_i, y_i) : 1 \leq i \leq n\}$  can be expressed by the power law

$$y_i \propto x_i^\beta \iff \ln y_i \sim \alpha + \beta \cdot \ln x_i, \quad \alpha, \beta \in \mathbb{R} \quad (25)$$

Let

$$\mathbf{A} = \begin{bmatrix} 1 & \ln(x_1) \\ 1 & \ln(x_2) \\ \vdots & \vdots \\ 1 & \ln(x_n) \end{bmatrix}, \quad \mathbf{p} = \begin{bmatrix} \alpha \\ \beta \end{bmatrix}, \quad \mathbf{b} = \begin{bmatrix} \ln(y_1) \\ \ln(y_2) \\ \vdots \\ \ln(y_n) \end{bmatrix}, \quad (26)$$

then the data set  $\{(x_i, y_i)\}$  specified by (25) can be expressed equivalently with the matrix-vector  $\langle \mathbf{A}, \mathbf{b} \rangle$  defined by (26). The procedure `FORMATPOWLAWDATA` listed in **Algorithm 2** is used for converting the primitive data set with power law to the matrix-vector pair  $\langle \mathbf{A}, \mathbf{b} \rangle$  with standard format.

---

**Algorithm 2** Converting primitive data set with power law to matrix-vector pair

---

**Input:** Vectors  $\mathbf{x}, \mathbf{y} \in \mathbb{R}^{n \times 1}$  such that  $y_i \propto x_i^\beta$ , sample capacity  $n \in \mathbb{N}$  for the data set.

**Output:** Pair  $\langle \mathbf{A}, \mathbf{b} \rangle$  such that  $\mathbf{A} = (a_{ij})_{2 \times n} \in \mathbb{R}^{2 \times n}$ ,  $\mathbf{b} = (b_i)_{n \times 1} \in \mathbb{R}^{n \times 1}$ ;

```

1: procedure FORMATPOWLAWDATA( $\mathbf{x}, \mathbf{y}, n$ )
2:    $\mathbf{A} \leftarrow \mathbf{0}_{2 \times n}$ ;
3:    $\mathbf{b} \leftarrow \mathbf{0}_{n \times 1}$ ;
4:   for  $i \in \langle 1, 2, \dots, n \rangle$  do
5:      $a_{i1} \leftarrow 1$ ;
6:      $a_{i2} \leftarrow \ln(x_i)$ ;
7:      $b_i \leftarrow \ln(y_i)$ ;
8:   end for
9:   return  $\langle \mathbf{A}, \mathbf{b} \rangle$ ;
10: end procedure

```

---

When the pair  $\langle \mathbf{A}, \mathbf{b} \rangle$  is created, we can establish the following standard over-determined linear system

$$\mathbf{A}\mathbf{p} = \mathbf{b}. \quad (27)$$

Thus, the parameter vector  $\mathbf{p} = [\alpha, \beta]^\top$  specified by the (27) can be estimated by solving the following convex optimization problem

$$\mathbf{p}_{\text{opt}} = \arg \min_{\mathbf{p} \in \mathbb{R}^{2 \times 1}} \|\mathbf{A}\mathbf{p} - \mathbf{b}\|_r, \quad r \in \mathbb{N} \quad (28)$$

where  $\|\mathbf{x}\|_r = \sqrt[r]{|x_1|^r + |x_2|^r + \dots + |x_m|^r}$  denotes the Euclidean norm of the  $m$ -dim vector  $\mathbf{x} \in \mathbb{R}^{m \times 1}$ . For  $r = 2$  in (28), we can take the *least squares* (LS) approach to solve for  $\mathbf{p}_{\text{opt}}$  by

$$\mathbf{p}_{\text{LS}} = \mathbf{A}^\dagger \mathbf{b} \quad (29)$$

where the  $\mathbf{A}^\dagger$  in (29) denotes the Moore-Penrose inverse of the matrix  $\mathbf{A}$  [42]. Various least squares methods can be attempted to obtain the minimum  $\ell_2$ -norm solution, such as *data least squares* (DLS), *total least squares* (TLS), and *scaled total least squares* (STLS) [43–45]. For better estimation property, the  $\ell_1$ -norm for the cost could be used in optimization with the help of residual vector [46].

In the sense of computer programming, the linear regression method of solving the parameter vector  $\mathbf{p}$  in (27) can be encapsulated into a procedure named by `LINEARREGRSOLVER` in order to be reused for different applications. The interface can be expressed by

$$\mathbf{p} \leftarrow \text{LINEARREGRSOLVER}(\mathbf{A}, \mathbf{b}, n, \text{flag}) \quad (30)$$

where the  $n$  in (30) is number of data and the `flag` is used for selecting the method for solving linear regression problem. For example, `flag = 2` implies the  $\ell_2$ -norm optimization and `flag = 1` implies the  $\ell_1$ -norm optimization.

## 2.7 Algorithm for Solving Fixed-Point in Euclidean Space

For the fixed-point equation

$$\mathbf{x} = T(f, \mathbf{x}, \lambda_1, \dots, \lambda_r), \quad \mathbf{x} \in \mathbb{R}^{m \times 1}$$

where  $T$  is a contractive mapping used as the *updating function* in programming language,  $\lambda_1, \dots, \lambda_r$  are possible extra parameters. The fixed-point can be solved with an iterative scheme [47]

$$\mathbf{x}_{i+1} = T(f, \mathbf{x}_i, \lambda_1, \dots, \lambda_r), \quad i = 0, 1, 2, \dots$$

when the initial value  $\mathbf{x}_0$  and the distance  $d(\mathbf{x}_{i+1}, \mathbf{x}_i)$ , such as the Euclidean norm, are provided properly according to the Cauchy's criteria for convergence.

The pseudo-code for the fixed-point algorithm is listed in **Algorithm 3**, in which the concepts of high order function and function object are utilized for the abstraction and flexibility. Note that the order of arguments can be configured by programmers.

---

**Algorithm 3** Unified Framework for Solving the Fixed-Point of  $\mathbf{x} = T(f, \mathbf{x}, \lambda_1, \dots, \lambda_r)$

---

**Input:** Contractive mapping  $T$  as the updatator which is a high order function, function object  $f$ , function object  $d$  for the distance  $d(\mathbf{x}_i, \mathbf{x}_{i+1})$ , precision  $\epsilon$ , initial value  $\mathbf{x}_{\text{guess}}$  and possible extra parameters  $\lambda_1, \dots, \lambda_r$  with the same or different data types.

**Output:** Fixed-point  $\mathbf{x}$  such that  $\mathbf{x} = T(f, \mathbf{x}, \lambda_1, \dots, \lambda_r)$

```

1: procedure FIXEDPOINTSOLVER( $T, f, d, \epsilon, \mathbf{x}_{\text{guess}}, \lambda_1, \dots, \lambda_r$ )
2:    $\mathbf{x}_{\text{improve}} \leftarrow T(f, \mathbf{x}_{\text{guess}}, \lambda_1, \dots, \lambda_r)$ ;
3:   while  $d(\mathbf{x}_{\text{improve}}, \mathbf{x}_{\text{guess}}) \geq \epsilon$  do
4:      $\mathbf{x}_{\text{guess}} \leftarrow \mathbf{x}_{\text{improve}}$ ;
5:      $\mathbf{x}_{\text{improve}} \leftarrow T(f, \mathbf{x}_{\text{guess}}, \lambda_1, \dots, \lambda_r)$ ;
6:   end while
7:   return  $\mathbf{x}_{\text{improve}}$ ;
8: end procedure

```

---

In the sense of programming language and discrete mathematics,  $f$  is an ordinary (first order) function,  $T$  is a second order function and FIXEDPOINTSOLVE is a third order function.

The procedure EUCLIDDIST described by **Algorithm 4** is designed for calculating the Euclidean distance. For our problem, we have  $d(x_i, x_{i+1}) = |x_i - x_{i+1}|$  since it is a 1-dim distance.

---

**Algorithm 4** Calculate the Euclidean distance of  $\mathbf{x}$  and  $\mathbf{y}$

---

**Input:**  $\mathbf{x}, \mathbf{y} \in \mathbb{R}^{m \times 1}$

**Output:** The Euclidean distance of  $\mathbf{x}$  and  $\mathbf{y}$ , i.e.,  $d(\mathbf{x}, \mathbf{y}) = \|\mathbf{x} - \mathbf{y}\|_2 = \sqrt{\sum_{i=1}^m |x_i - y_i|^2}$ .

```

1: procedure EUCLIDDIST( $\mathbf{x}, \mathbf{y}$ )
2:    $\text{sum} \leftarrow 0$ ;
3:   for  $i \in \langle 1, \dots, m \rangle$  do
4:      $\text{sum} \leftarrow \text{sum} + |x_i - y_i|^2$ ;
5:   end for
6:    $\text{dist} \leftarrow \sqrt{\text{sum}}$ ; // it will be  $d(x, y) = |x - y|$  if  $m = 1$ ;
7:   return  $\text{dist}$ ;
8: end procedure

```

---

## 2.8 Algorithm for Searching a Local Minimum of Single-variable Function

In 2013, Brent [48] provides a line-search method which is a combination of golden section search and successive parabolic interpolation. It can be used for finding a local minimum of a single-variable function, please see the **Algorithm 24** in Appendix A for details.

### 3 Optimal Sequence Partition

#### 3.1 Fundamental Operations on Time Sequences

##### 3.1.1 Cumulative Sum of Sequence

For a sequence  $\{x_i : 1 \leq i \leq n\}$ , its cumulative sequence  $\{c_i : 1 \leq i \leq n\}$  is defined by the action of cumulative sum operator on the original sequence. Formally, we have

$$c_i = \mathcal{C}_j^{1:i} \{x_j\} = \sum_{j=1}^i x_j, \quad 1 \leq i \leq n. \quad (31)$$

In consequence, the relation between the cumulative sum operator and arithmetic average operator is

$$\mathcal{A}_j^{1:i} \{x_j\} = \frac{1}{i} \cdot \mathcal{C}_j^{1:i} \{x_j\}, \quad 1 \leq i \leq n. \quad (32)$$

Logically, the cumulative sum is more fundamental than the arithmetic average. Note that (31) and (32) can be deduced from (3) directly.

Particularly, for the time sequence  $\{X_t : 1 \leq t \leq N\}$ , its cumulative sequence is

$$\mathcal{C}_j^{1:i} \{X_j\} = \sum_{j=1}^i X_j, \quad 1 \leq i \leq n \quad (33)$$

and its cumulative bias sequence is

$$\mathcal{C}_j^{1:i} \{X_j - \bar{X}\} = \sum_{j=1}^i (X_j - \bar{X}), \quad 1 \leq i \leq n \quad (34)$$

where the  $\bar{X} = \mathcal{A}_t^{1:n} \{X_t\}$  in (34) is the global arithmetic average as described in (4). The equations (33) and (34) will be encountered frequently when constructing the estimator of Hurst exponent.

##### 3.1.2 Sequence Partition

For computing the Hurst exponent, it is valuable to split the original sequence into several subsequences and construct the statistics of interest.

A fundamental task is to find a suitable length for the subsequence, which helps in efficiently splitting the sequence as well as preserving the intrinsic characteristics.

A time sequence  $\mathbf{X} = \{X_t\}_{t=1}^N$  with length  $N$  can be partitioned into  $k$  subsequences or segments of equal size  $m$  such that

$$N = km + r, \quad k = \lfloor N/m \rfloor.$$

If  $m \nmid N$  or equivalently  $r \neq 0$ , we just ignore the following subsequence with length  $r \in \{1, 2, \dots, m-1\}$ , viz.

$$\{X_{km+1}, X_{km+2}, \dots, X_{km+r}\}, \quad 1 \leq r \leq m-1.$$

The  $k$  subsequences of size  $m$  obtained can be expressed by

$$\bigcup_{\tau=1}^k X_{(\tau)} = \{X_{(\tau)} : 1 \leq \tau \leq k\} \quad (35)$$

where

$$\begin{aligned} X_{(\tau)} &= \{X_{(\tau-1)m+j} : 1 \leq j \leq m\}, \quad 1 \leq \tau \leq k \\ &= \{X_{(\tau-1)m+1}, \dots, X_{(\tau-1)m+j}, \dots, X_{(\tau-1)m+m}\} \end{aligned} \quad (36)$$

is the  $\tau$ -th subsequence. For simplicity, we can denote the partition operation of the sequence  $\mathbf{X}$  as

$$\{X_{(\tau)} : 1 \leq \tau \leq k\} = \text{SEPARTITION}(\mathbf{X}, m, k) \quad (37)$$

according to (36). Equation (37) can be used to simplify the software implementation of sequence partition.

## 3.2 Steps and Algorithms for Optimal Sequence Partition

### 3.2.1 Steps for Optimal Sequence Partition

According to (35), the partition of  $\{X_t : 1 \leq N\}$  depends on the size  $m$  for the subsequences. It is a key issue that how to specify the size  $m$ . There are three steps for determining the positive integer  $m$ :

- generating the set of bounded proper factors for the candidate length and calculating the cardinality of the set;
- searching an optimal length for replacing the original sequence length;
- set the  $m$  in the bounded proper factors of the optimal length.

### 3.2.2 Brute-force Searching Method for Specifying Bounded Proper Factors of Composite Integer

The procedure GENSBBPF listed in **Algorithm 5** is designed for finding the set of bounded proper factors of a composite  $a$  specified by the integer  $w \in \{2, \dots, \lfloor \sqrt{a} \rfloor\}$ .

---

**Algorithm 5** Generate the set of bounded proper factors of the composite  $a \in \mathbb{N}$  with the lower bound  $w$  and the upper bound  $a/w$  such that  $w \in \{2, \dots, \lfloor \sqrt{a} \rfloor\}$  with the brute-force searching method.

---

**Input:** Composite number  $a \in \mathbb{N}$ , lower bound  $w \in \{2, 3, \dots, \lfloor \sqrt{a} \rfloor\}$ .

**Output:** The set  $S_{\text{bpf}}(a, w)$ .

```

1: procedure GENSBBPF( $a, w$ )
2:    $S_{\text{bpf}} \leftarrow \emptyset$ ;
3:   for  $i \in \langle w, w + 1, \dots, \lfloor a/w \rfloor \rangle$  do
4:     if  $i \mid a$  then
5:        $S_{\text{bpf}} \leftarrow S_{\text{bpf}} \cup \{i\}$ ;
6:     end if
7:   end for
8:   return  $S_{\text{bpf}}$ ;
9: end procedure

```

---

### 3.2.3 Searching Optimal Approximate Length of Sequence

The procedure SEARCHOPTSEQLEN for searching the optimal length for the subsequence is listed in **Algorithm 6**.

---

**Algorithm 6** Searching the optimal length of sequence.

---

**Input:** Sequence length  $N$ , lower bound  $w \in \{2, \dots, \lfloor \sqrt{N} \rfloor\}$ , percentage  $\alpha \in [0.95, 1]$  with default value  $\alpha = 0.99$ .

**Output:** Optimal sequence length  $N_{\text{opt}}$  such that  $N_{\text{opt}} \leq N$  and  $S_{\text{bpf}}(N_{\text{opt}})$  is not empty.

```

1: procedure SEARCHOPTSEQLEN( $N, w, \alpha$ )
2:    $L_{\text{factors}} \leftarrow \emptyset$ ; // initialize with empty set
3:    $n_0 \leftarrow \lceil \alpha N \rceil$ ;
4:   for  $i \in \langle n_0, n_0 + 1, \dots, N \rangle$  do
5:      $S_{\text{bpf}} \leftarrow \text{GENSBBPF}(i, w)$ ;
6:      $L_{\text{factors}} \leftarrow L_{\text{factors}} \cup |S_{\text{bpf}}|$ ;
7:   end for
8:    $\langle i_{\text{max}}, v_{\text{max}} \rangle \leftarrow \text{SEARCHMAX}(L_{\text{factors}})$ ;
9:    $N_{\text{opt}} \leftarrow n_0 + i_{\text{max}} - 1$ ;

```

10: **return**  $N_{\text{opt}}$ ;  
11: **end procedure**

### 3.2.4 Specifying the Parameters of Subsequence

The  $N_{\text{opt}}$  obtained from the length  $N$  must be a composite number. The set of bounded proper factors of  $N_{\text{opt}}$  with lower bound  $w$  gives the possible values for the size  $m$  required in sequence partition. In other words, we have

$$m \in S_{\text{bpf}}(N_{\text{opt}}, w). \quad (38)$$

Once the size  $m$  specified by (38) is obtained, the  $k = N_{\text{opt}}/m$  will be determined simultaneously. In consequence, the sequence partition is specified completely. As an illustration, we take  $N = 997$ ,  $w = 20$ ,  $\alpha = 0.99$ , which implies  $N_{\text{opt}} = 990$  by **Algorithm 6**. Consequently,

$$S_{\text{bpf}}(N_{\text{opt}}, w) = S_{\text{bpf}}(990, 22) = \{22, 30, 33, 45\}.$$

This implies that there are four candidate values for the pair  $\langle m, k \rangle$  of interest, i.e.

$$\langle m, k \rangle \in \{\langle 22, 45 \rangle, \langle 30, 33 \rangle, \langle 33, 30 \rangle, \langle 45, 22 \rangle\}.$$

**Figure 2** demonstrates the principle and implementation of optimal sequence partition intuitively.

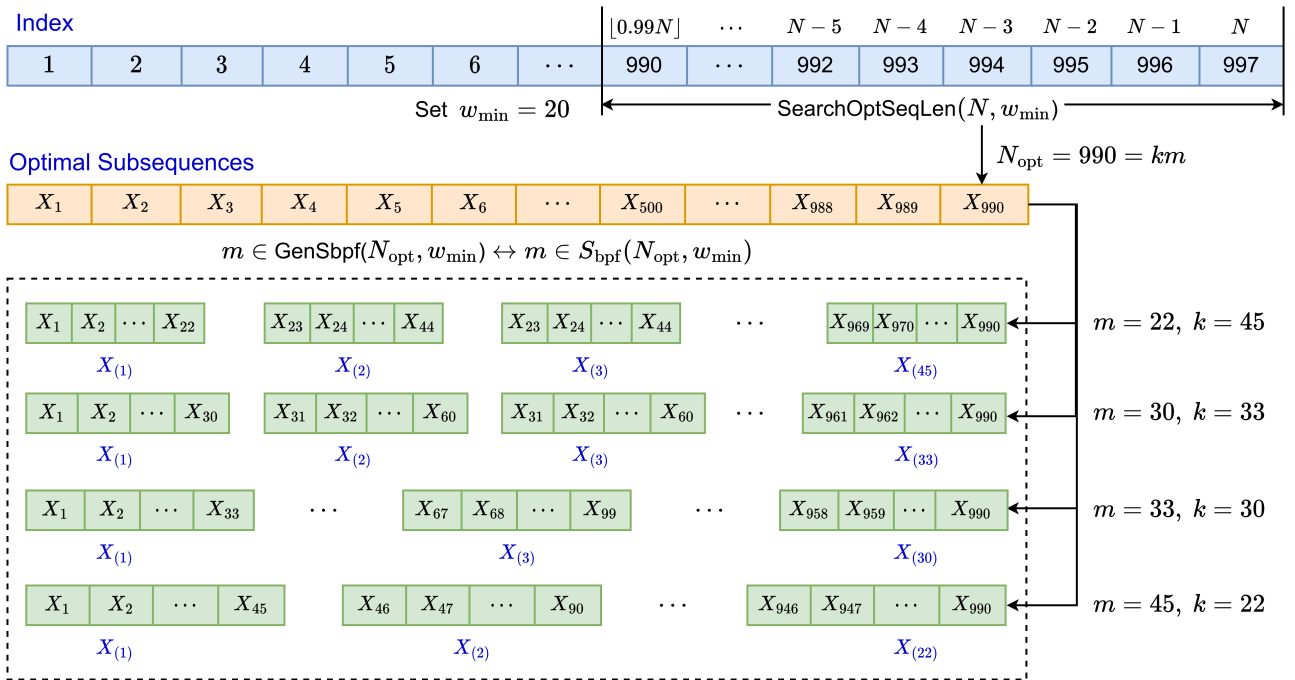


Figure 2: Principle and implementation of optimal sequence partition

## 4 Typical Methods For Estimating Hurst Exponent

There are various algorithms for estimating the Hurst exponent  $H$  of time sequences based on different principles. For the convenience of various applications, it is necessary to describe the algorithms with pseudo-codes and provide the code for the implementation with popular high level programming languages such as C/C++, Python and Octave/MATLAB. In this section, we will cope with the principles briefly and present pseudo-codes for the algorithms for the estimation methods. We remark that our emphasis is put on the understandability of the principle and the usability of the algorithms for estimating the Hurst exponent of TS.

## 4.1 Central Estimation

### 4.1.1 Principle of Central Estimator

For the time sequence  $\mathbf{X} = \{X_t : 1 \leq t \leq N\}$ , we can decompose it into  $k$  subsequences with segment size  $m$  by (35). Now we compute the moment for each subsequence. Let

$$C_\tau = \mathcal{A}_j^{1:m} \{X_{(\tau-1)m+j}\}, \quad 1 \leq \tau \leq k, \quad (39)$$

then the  $C_\tau$  in (39) is the arithmetic average of the subsequence  $X_{(\tau)}$ . Thus we get a new sequence  $\{C_\tau : 1 \leq \tau \leq k\}$ . The  $r$ -th central moment of this sequence can be written by

$$\nu(r, m) = \mathcal{A}_\tau^{1:k} \{|C_\tau - \bar{X}|^r\}. \quad (40)$$

where  $\bar{X}$  in (40) is specified by (4). If the sequence  $\{X_t\}_{t=1}^N$  is a Gaussian sequence or its variance is finite, then for large  $k$  and  $m$  the asymptotic property

$$\nu(r, m) \propto m^{r(H-1)} \quad (41)$$

holds [49]. Obviously, (41) means a typical example of power law presented in (25). By taking the logarithms of both sides of (41) we immediately have

$$\ln \nu(r, m) \sim \alpha_{\text{Central}}(r) + \beta_{\text{Central}}(r) \cdot \ln m \quad (42)$$

where

$$\beta_{\text{Central}}(r) = r(H-1). \quad (43)$$

Substituting (43) into (42), we can get the estimator

$$\hat{H}_{\text{Central}}(r) = 1 + \frac{1}{r} \hat{\beta}_{\text{Central}}(r), \quad (44)$$

for the Hurst exponent, which can be obtained with the linear regression. Particularly, for  $r = 1$  and  $r = 2$ , we have two subtypes of estimation method:

- (1) **Absolute Moments** (AM) method [5], in which  $r = 1$  and we have

$$\hat{H}_{\text{AM}} = \hat{H}_{\text{Central}}(1) = 1 + \hat{\beta}_{\text{Central}}(1). \quad (45)$$

- (2) **Aggregate Variance** (AV) method [5], in which  $r = 2$  and we have

$$\hat{H}_{\text{AV}} = \hat{H}_{\text{Central}}(2) = 1 + \frac{1}{2} \hat{\beta}_{\text{Central}}(2). \quad (46)$$

Obviously, (45) and (46) are special cases of (44).

### 4.1.2 Algorithm for Central Estimator

The key step of central estimation is constructing the corresponding central moments  $\nu(r, m)$  according to (40). The procedure ESTHURSTCENTRAL listed in **Algorithm 7** is used to estimate the Hurst exponent by (39), (40), (41), (42), (43) and (44), which relies on two procedures:

- the procedures GENSBPF listed in **Algorithm 5** for generating factor set, and
- the procedure SEARCHOPTSEQLEN listed in **Algorithm 6** for searching the optimal sequence length.

For time-domain methods, the parameter estimation for linear model is fundamental for the estimation, please see the subsection 2.6 about linear regression.

---

**Algorithm 7** Central Estimator for Hurst exponent

---

**Input:** Time sequence  $\mathbf{X}$ , window size  $w$ , order  $r \in \{1, 2\}$ , indicator **flag** for the optimization method in linear regression.

**Output:** Hurst exponent of the sequence  $\mathbf{X}$ .

```

1: procedure ESTHURSTCENTRAL( $\mathbf{X}, w, r, \text{flag}$ )
2:    $N \leftarrow \text{GETLENGTH}(\mathbf{X});$ 
3:    $N_{\text{opt}} \leftarrow \text{SEARCHOPTSEQLEN}(N, w);$ 
4:    $\mathbf{T} \leftarrow \text{GENSBPF}(N_{\text{opt}}, w);$  //  $S_{\text{bpf}}(N_{\text{opt}}, w)$ 
5:    $n \leftarrow \text{GETLENGTH}(\mathbf{T});$  //  $|S_{\text{bpf}}(N_{\text{opt}}, w)|$ 
6:    $\mathbf{S} \leftarrow \mathbf{0} \in \mathbb{R}^{n \times 1};$  // For the statistics
7:    $\bar{\mathbf{X}} \leftarrow \mathcal{A}_t^{1:N} \{X_t\};$ 
8:   for  $\text{idx} \in \langle 1, 2, \dots, n \rangle$  do
9:      $m \leftarrow T_{\text{idx}};$  //  $m$  is the interval time
10:     $k \leftarrow \lfloor N_{\text{opt}}/m \rfloor;$  // number of subsequences
11:     $\mathbf{Y} \leftarrow \mathbf{0} \in \mathbb{R}^{k \times 1};$  //  $\mathbf{Y} = [Y_1, \dots, Y_\tau, \dots, Y_k]^\top;$ 
12:     $\{X_\tau : 1 \leq \tau \leq k\} \leftarrow \text{SEQPARTITION}(\mathbf{X}, N, m);$ 
13:    for  $\tau \in \{1, 2, \dots, k\}$  do
14:       $Y_\tau \leftarrow \mathcal{A}_j^{1:m} \{X_{(\tau-1)m+j}\};$  // arithmetic ave
15:    end for
16:    if  $r = 1$  then
17:       $\nu \leftarrow \|\mathbf{Y} - \bar{\mathbf{X}}\|_1/k;$  //  $\ell_1$ -norm here
18:    else
19:       $\nu \leftarrow \text{Var}(\mathbf{Y});$  //  $r = 2$ 
20:    end if
21:     $S_{\text{idx}} \leftarrow \nu;$ 
22:  end for
23:   $\langle \mathbf{A}, \mathbf{b} \rangle \leftarrow \text{FORMATPOWLAWDATA}(\mathbf{T}, \mathbf{S}, n);$ 
24:   $\mathbf{p} \leftarrow \text{LINEARREGRSOLVER}(\mathbf{A}, \mathbf{b}, n, \text{flag});$  // by (30)
25:   $\beta_{\text{Central}} \leftarrow p_2;$  //  $\mathbf{p} = [\alpha, \beta]^\top;$ 
26:   $H \leftarrow \beta_{\text{Central}}/r + 1;$ 
27:  return  $H;$ 
28: end procedure

```

---

## 4.2 Generalized Hurst Exponent Method (GHE)

### 4.2.1 Principle of GHE Estimator

For time sequence  $\{X_t\}_{t=1}^N$ , the  $q$ -th order moment of the distribution of the increments based on the time lag  $\tau$  can be written by [6]

$$\mu_q(\tau) = \mathcal{A}_i^{1:N-\tau} \{|X_{i+\tau} - X_i|^q\} \quad (47)$$

The *generalized Hurst exponent* (GHE), denoted by  $H(q)$ , can be deduced from the asymptotic scaling behavior of (47), viz. [50]

$$\mu_q(\tau) \propto \tau^{qH(q)} \iff \ln \mu_q(\tau) \sim \alpha_{\text{GHE}} + \beta_{\text{GHE}} \cdot \ln \tau \quad (48)$$

Obviously, (48) is a special case of the equivalent form of power law specified by (25). In consequence, the generalized Hurst exponent  $H(q)$  can be expressed by [50]

$$\hat{H}_{\text{GHE}} = \frac{\hat{\beta}_{\text{GHE}}}{q}. \quad (49)$$

## 4.2.2 Algorithm for GHE Estimator

The procedure ESTHURSTGHE described in **Algorithm 8** can be used to compute the Hurst exponent based on (47), (48) and (49).

---

### Algorithm 8 Generalized Hurst Exponent Method

---

**Input:** Time series data  $\mathbf{X}$ , order  $q$ , indicator **flag** for the optimization method in linear regression.

**Output:** Hurst exponent of the sequence  $\mathbf{X}$ .

```

1: procedure ESTHURSTGHE( $\mathbf{X}, q, \text{flag}$ )
2:    $n \leftarrow 10$ ;
3:    $N \leftarrow \text{GETLENGTH}(\mathbf{X})$ ;
4:    $\mathbf{T} \leftarrow [1, 2, \dots, n]^T \in \mathbb{R}^{n \times 1}$ ;
5:    $\mathbf{S} \leftarrow \mathbf{0} \in \mathbb{R}^{n \times 1}$ ; // For the statistics
6:    $\bar{X} \leftarrow \mathcal{A}_i^{1:N} \{X_i\}$ ;
7:    $\mathbf{Y} \leftarrow \mathbf{0} \in \mathbb{R}^{N \times 1}$ ;
8:   for  $i \in \langle 1, 2, \dots, N \rangle$  do
9:      $Y_i \leftarrow \mathcal{C}_j^{1:i} \{X_j - \bar{X}\}$ ; // by (34)
10:  end for
11:  for  $\text{idx} \in \langle 1, 2, \dots, n \rangle$  do
12:     $\mu_q \leftarrow \mathcal{A}_i^{1:N-\text{idx}} \{|Y_{i+\text{idx}} - Y_i|^q\}$ ; // by (47)
13:     $S_{\text{idx}} \leftarrow \mu_q$ ;
14:  end for
15:   $\langle \mathbf{A}, \mathbf{b} \rangle \leftarrow \text{FORMATPOWLAWDATA}(\mathbf{T}, \mathbf{S}, n)$ ;
16:   $\mathbf{p} \leftarrow \text{LINEARREGRSOLVER}(\mathbf{A}, \mathbf{b}, n, \text{flag})$ ;
17:   $\beta_{\text{GHE}} \leftarrow p_2$ ; //  $\mathbf{p} = [\alpha, \beta]^T$ ;
18:   $H \leftarrow \beta_{\text{GHE}}/q$ ; // by (49)
19:  return  $H$ ;
20: end procedure

```

---

## 4.3 Higuchi Method (HM)

### 4.3.1 Principle of Higuchi Estimator

For the time sequence  $\{X_t\}_{t=1}^N$ , its cumulative bias sequence is defined by [5]

$$Y_i = \mathcal{C}_j^{1:i} \{X_j - \bar{X}\}, \quad 1 \leq i \leq N \quad (50)$$

where  $\bar{X} = \mathcal{A}_t^{1:N} \{X_t\}$  and the normalized length of each sample

$$L_k(m) = \frac{\gamma}{m} \sum_{i=1}^{\lfloor (N-k)/m \rfloor} |Y_{k+im} - Y_{k+(i-1)m}|, \quad 1 \leq k \leq m \quad (51)$$

can be calculated with the help of (50), where the integers  $k$  and  $m$  indicate the initial time and the interval time respectively. The normalization factor  $\gamma$  in (51) is defined by

$$\gamma = \frac{N-1}{\lfloor (N-k)/m \rfloor \cdot m}. \quad (52)$$

Higuchi showed that [7]

$$L(m) = \mathcal{A}_k^{1:m} \{L_k(m)\} \propto m^{-D} \iff \ln L(m) \sim \alpha_{\text{HM}} + \beta_{\text{HM}} \ln m \quad (53)$$

where the parameter  $D$  is the fractal dimension of the time sequence and  $\beta_{\text{HM}} = -D$ . Obviously, (53) is a special case of the equivalent form of power law specified by (25). Substituting the (10) into (53), we can obtain the Higuchi estimator

$$\hat{H}_{\text{HM}} = 2 + \hat{\beta}_{\text{HM}}. \quad (54)$$

for the Hurst exponent according to (53).

### 4.3.2 Algorithm for Higuchi Estimator

The procedure ESTHURSTHIGUCHI described **Algorithm 9** is designed for estimating the Hurst exponent based on (50), (51), (52),(53) and (54).

---

**Algorithm 9** Higuchi method for estimating the Hurst exponent

---

**Input:** Time series data  $\mathbf{X}$ , indicator **flag** for the optimization method in linear regression.

**Output:** Hurst exponent of the sequence  $\mathbf{X}$ .

```

1: procedure ESTHURSTHIGUCHI( $\mathbf{X}$ , flag)
2:    $n \leftarrow 10$ ;
3:    $N \leftarrow \text{GETLENGTH}(\mathbf{X})$ ;
4:    $\mathbf{T} \leftarrow \mathbf{0} \in \mathbb{R}^{n \times 1}$ ; // For the interval time
5:    $\mathbf{S} \leftarrow \mathbf{0} \in \mathbb{R}^{n \times 1}$ ; // For the statistics
6:    $\bar{X} \leftarrow \mathcal{A}(X_i)$ ;
7:    $\mathbf{Y} \leftarrow \mathbf{0} \in \mathbb{R}^{N \times 1}$ ;
8:   for  $i \in \langle 1, 2, \dots, N \rangle$  do
9:      $Y_i \leftarrow \mathcal{C}_j^{1:i} \{X_j - \bar{X}\}$ ; // by (50)
10:  end for
11:  for  $\text{idx} \in \langle 1, 2, \dots, n \rangle$  do
12:    if  $\text{idx} > 4$  then
13:       $m \leftarrow \lfloor 2^{(\text{idx}+5)/4} \rfloor$ ;
14:    else
15:       $m \leftarrow \text{idx}$ ;
16:    end if
17:     $T_{\text{idx}} \leftarrow m$ ;
18:     $k \leftarrow \lfloor N/m \rfloor$ ;
19:     $L_k \leftarrow \mathcal{A}_i^{1:k-1} \left\{ \mathcal{A}_j^{(i-1)m+1:im} \{|Y_{j+m} - Y_j|\} \right\}$ ;
20:     $S_{\text{idx}} \leftarrow (N-1) \cdot L_k/m^2$ ; // by (51) and (52)
21:  end for
22:   $\langle \mathbf{A}, \mathbf{b} \rangle \leftarrow \text{FORMATPOWLAWDATA}(\mathbf{T}, \mathbf{S}, n)$ ;
23:   $\mathbf{p} \leftarrow \text{LINEARREGRSOLVER}(\mathbf{A}, \mathbf{b}, n, \text{flag})$ ;
24:   $\beta_{\text{HM}} \leftarrow p_2$ ; //  $\mathbf{p} = [\alpha, \beta]^T$ ;
25:   $H \leftarrow \beta_{\text{HM}} + 2$ ; // by (54)
26:  return  $H$ ;
27: end procedure

```

---

## 4.4 Detrended Fluctuation Analysis (DFA)

### 4.4.1 Principle of DFA Estimator

The DFA method for computing the Hurst exponent is based on the sequence partition. For the time sequence  $\{X_t\}_{t=1}^N$ , with the configuration of parameter  $\alpha \in [0.95, 1]$  and minimal size  $w$  of the subsequence, then optimal sequence length  $N_{\text{opt}}$  can be solved with **Algorithm 6**, the size  $m$  can be calculated by (38) and the number of subsequence will be  $k = N_{\text{opt}}/m$ .

For the purpose of clarity and intuition, the principle DFA method is shown in **Figure 3**. We now give some interpretations for the steps for the DFA estimator:

0) Pre-conditioning:

Partitioning the sequence  $\{X_t : 1 \leq t \leq N\}$  into  $k$  subsequences with minimal size  $w$  such that  $N_{\text{opt}} = mk$  and  $m \in S_{\text{bpf}}(N_{\text{opt}}, w) = \{m_1, m_2, \dots, m_n\}$  where  $n = |S_{\text{bpf}}(N_{\text{opt}}, w)|$ .

i) Computing the global arithmetic average of the optimal sequence  $\{X_t : 1 \leq t \leq N_{\text{opt}} = mk\}$  by

$$\overline{X_{\text{opt}}} = \mathcal{A}_t^{1:N_{\text{opt}}} \{X_t\} \quad (55)$$

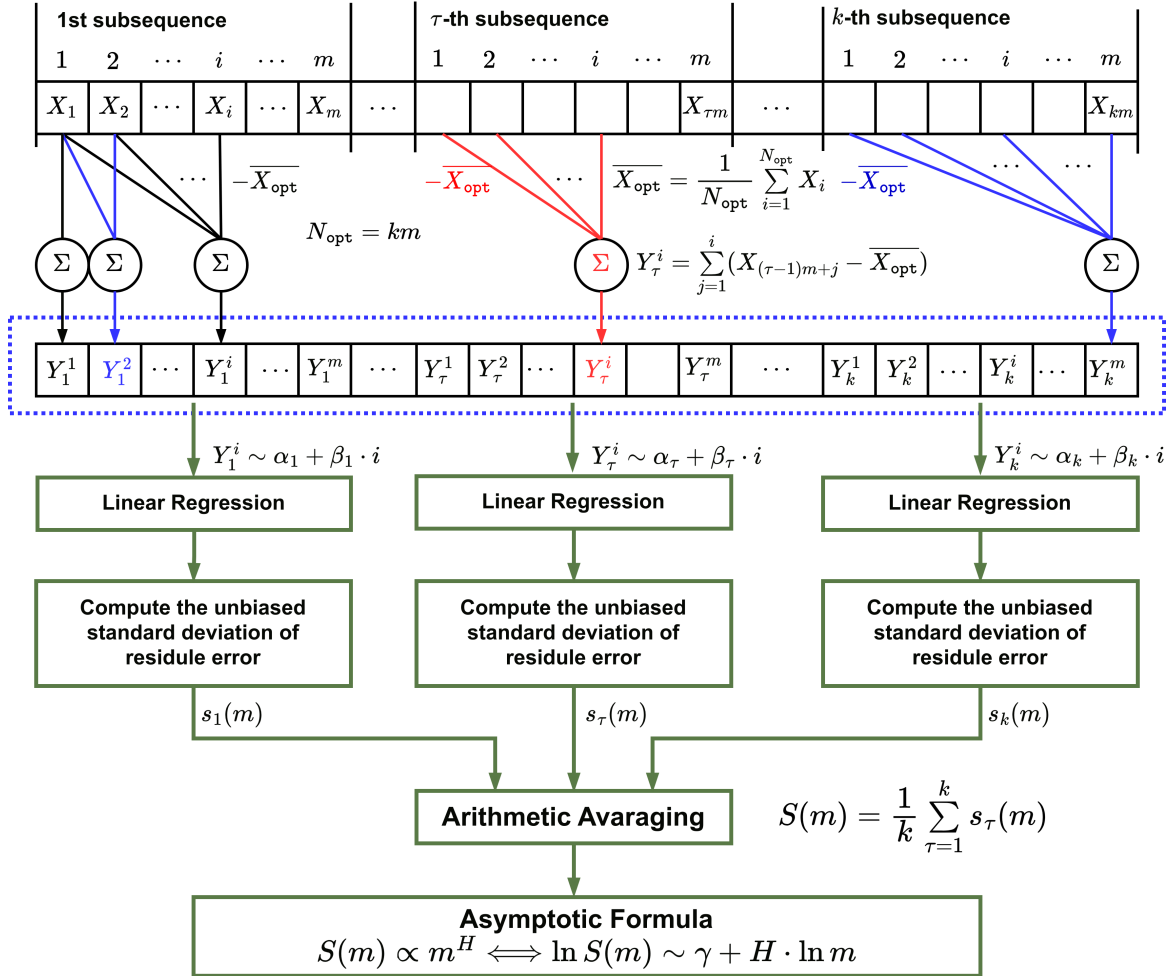


Figure 3: Partition of time sequence and structure of cumulative sequence for DFA method

and construct the cumulative bias sequence

$$Z_i = \mathcal{C}_j^{1:i} \{X_j - \overline{X_{\text{opt}}}\}, \quad 1 \leq i \leq N_{\text{opt}}. \quad (56)$$

ii) Constructing the  $k$  subsequences  $\{Y_\tau^i : 1 \leq i \leq m\}$  for  $1 \leq \tau \leq k$  by

$$\mathbf{Y}_\tau = [Y_\tau^1, Y_\tau^2, \dots, Y_\tau^m]^\top, \quad 1 \leq \tau \leq k \quad (57)$$

where

$$Y_\tau^i = Z_{(\tau-1)m+i}, \quad 1 \leq i \leq m. \quad (58)$$

iii) Performing the linear regression for each subsequence  $\{Y_\tau^i : 1 \leq i \leq m\}$  specified by (55) for  $1 \leq \tau \leq k$  [51, 52]

$$Y_\tau^i \sim \alpha_\tau + \beta_\tau \cdot i, \quad 1 \leq i \leq m \quad (59)$$

or equivalently

$$\mathbf{q}_\tau \leftarrow \text{LINEARREGRSOLVER}(\mathbf{M}, \mathbf{Y}_\tau, m, \text{flag}) \quad (60)$$

for  $\mathbf{q}_\tau = [\alpha_\tau, \beta_\tau]^\top$  such that

$$\mathbf{M} = \begin{bmatrix} 1 & 1 & \dots & 1 \\ 1 & 2 & \dots & m \end{bmatrix}^\top, \quad \boldsymbol{\varepsilon}_\tau = \mathbf{Y}_\tau - \mathbf{M}\mathbf{q}_\tau \quad (61)$$

or equivalent in the component form

$$\varepsilon_\tau^i = Y_\tau^i - \alpha_\tau - \beta_\tau \cdot i, \quad 1 \leq i \leq m. \quad (62)$$

iv) Calculating the unbiased standard deviation of the residual sequence

$$s_\tau(m) = \mathcal{S}_i^{1:m} \{\varepsilon_\tau^i\}. \quad (63)$$

v) Calculating the arithmetic average of each standard deviation

$$S(m) = \mathcal{A}_\tau^{1:k} \{s_\tau(m)\}. \quad (64)$$

in order to get the asymptotic relation

$$S(m) \propto m^H \iff \ln S(m) \sim \gamma + H \cdot \ln m \quad (65)$$

vi) Repeating the steps i) ~ v) for  $n$  times for different choices of  $m$  and setting

$$\begin{cases} \mathbf{T} = [m_1, \dots, m_n]^\top \\ \mathbf{S} = [S(m_1), \dots, S(m_n)]^\top \\ \langle \mathbf{A}, \mathbf{b} \rangle \leftarrow \text{FORMATPOWLAWDATA}(\mathbf{T}, \mathbf{S}, n) \end{cases}$$

vii) Estimating the Hurst exponent with linear regression

$$\mathbf{p}_{\text{DFA}} \leftarrow \text{LINEARREGRSOLVER}(\mathbf{A}, \mathbf{b}, k, \text{flag})$$

where  $\mathbf{p}_{\text{DFA}} = [\hat{\alpha}_{\text{DFA}}, \hat{\beta}_{\text{DFA}}]^\top$ , which implies that

$$\hat{H}_{\text{DFA}} = \hat{\beta}_{\text{DFA}}.$$

#### 4.4.2 Algorithm for DFA Estimator

The curve fitting method is a crucial step in the DFA-method, we need to frequently solve for the slope and intercept to construct the corresponding residual vectors. The **Algorithm 10** is designed to compute the Hurst exponent with the DFA estimator based on (55), (56), (57), (58), (59), (60), (61), (62), (63), (64) and (65).

---

**Algorithm 10** Detrended Fluctuation Analysis Estimator for Hurst exponent

---

**Input:** Time sequence  $\mathbf{X}$ , window size  $w$ , indicator **flag** for the optimization method in linear regression.

**Output:** Hurst exponent of the sequence  $\mathbf{X}$ .

```

1: procedure ESTHURSTDFA( $\mathbf{X}, w, \mathbf{flag}$ )
2:    $N \leftarrow \text{GETLENGTH}(\mathbf{X});$ 
3:    $N_{\text{opt}} \leftarrow \text{SEARCHOPTSEQLEN}(N, w);$ 
4:    $\mathbf{T} \leftarrow \text{GENSBPF}(N_{\text{opt}}, w);$  //  $S_{\text{bpf}}(N_{\text{opt}}, w)$ 
5:    $n \leftarrow \text{GETLENGTH}(\mathbf{T});$  //  $|S_{\text{bpf}}(N_{\text{opt}}, w)|$ 
6:    $\mathbf{S} \leftarrow \mathbf{0} \in \mathbb{R}^{n \times 1};$  // For the statistics
7:    $\mathbf{Z} \leftarrow \mathbf{0} \in \mathbb{R}^{N \times 1};$  // global cumulative sequence
8:    $\overline{X}_{\text{opt}} \leftarrow \mathcal{A}_i^{1:N_{\text{opt}}} \{X_i\};$  // global arithmetic average
9:   for  $i \in \langle 1, 2, \dots, N \rangle$  do
10:     $Z_i \leftarrow \mathcal{C}_j^{1:i} \{X_j - \overline{X}_{\text{opt}}\};$ 
11:  end for
12:  for  $\text{idx} \in \langle 1, 2, \dots, n \rangle$  do
13:     $m \leftarrow T_{\text{idx}};$ 
14:     $k \leftarrow N_{\text{opt}}/m;$ 
15:     $\mathbf{s}_\tau \leftarrow \mathbf{0} \in \mathbb{R}^{k \times 1};$  // vector of standard deviation
16:     $\boldsymbol{\varepsilon}_\tau \leftarrow \mathbf{0} \in \mathbb{R}^{m \times 1};$  // vector of regression residuals
17:     $\mathbf{M} \leftarrow \begin{bmatrix} 1 & 1 & \dots & 1 \\ 1 & 2 & \dots & m \end{bmatrix}^\top;$  // for linear regression
18:     $\mathbf{q}_\tau \leftarrow \mathbf{0} \in \mathbb{R}^{2 \times 1};$  //  $\mathbf{q} = [\alpha, \beta]^\top$ 
19:    for  $\tau \in \langle 1, 2, \dots, k \rangle$  do
20:       $\mathbf{Y}_\tau \leftarrow [Z_{(\tau-1)m+1}, Z_{(\tau-1)m+2}, \dots, Z_{\tau m}]^\top;$ 
21:       $\mathbf{q}_\tau \leftarrow \text{LINEARREGRESSION}(\mathbf{M}, \mathbf{Y}_\tau, m, \mathbf{flag});$ 
22:       $\boldsymbol{\varepsilon}_\tau \leftarrow \mathbf{Y}_\tau - \mathbf{M}\mathbf{q}_\tau;$ 
23:       $s_\tau \leftarrow \mathcal{S}_i^{1:m} \{\boldsymbol{\varepsilon}_\tau^i\};$ 
24:    end for
25:     $S_{\text{idx}} \leftarrow \mathcal{A}_\tau^{1:k} \{s_\tau\};$ 
26:  end for
27:   $\langle \mathbf{A}, \mathbf{b} \rangle \leftarrow \text{FORMATPOWLAWDATA}(\mathbf{T}, \mathbf{S}, n);$ 
28:   $\mathbf{p} \leftarrow \text{LINEARREGRSOLVER}(\mathbf{A}, \mathbf{b}, n, \mathbf{flag});$ 
29:   $\beta_{\text{DFA}} \leftarrow p_2;$  //  $\mathbf{p} = [\alpha, \beta]^\top;$ 
30:   $H \leftarrow \beta_{\text{DFA}};$ 
31:  return  $H;$ 
32: end procedure

```

---

It should be noted that in **Algorithm 10**, we have taken a strategy of cumulative calculation over the entire sequence. By comparing with the operation of cumulative calculation for each samples as described in equation (58), this approach can reduce the computational complexity significantly.

## 4.5 Rescaled Range Analysis (R/S Analysis)

### 4.5.1 Principle of R/S Estimator

Similar to the DFA method, for the time sequence  $\{X_t\}_{t=1}^N$ , with the configuration of parameter  $\alpha \in [0.95, 1]$  and minimal size  $w$  of the subsequence, the optimal sequence length  $N_{\text{opt}}$  can be solved with **Algorithm 6**, the size  $m$  can be calculated by (38) and the number of subsequence will be  $k = N_{\text{opt}}/m$ . The way for finding the Hurst exponent [52] by R/S method is illustrated in **Figure 4**.

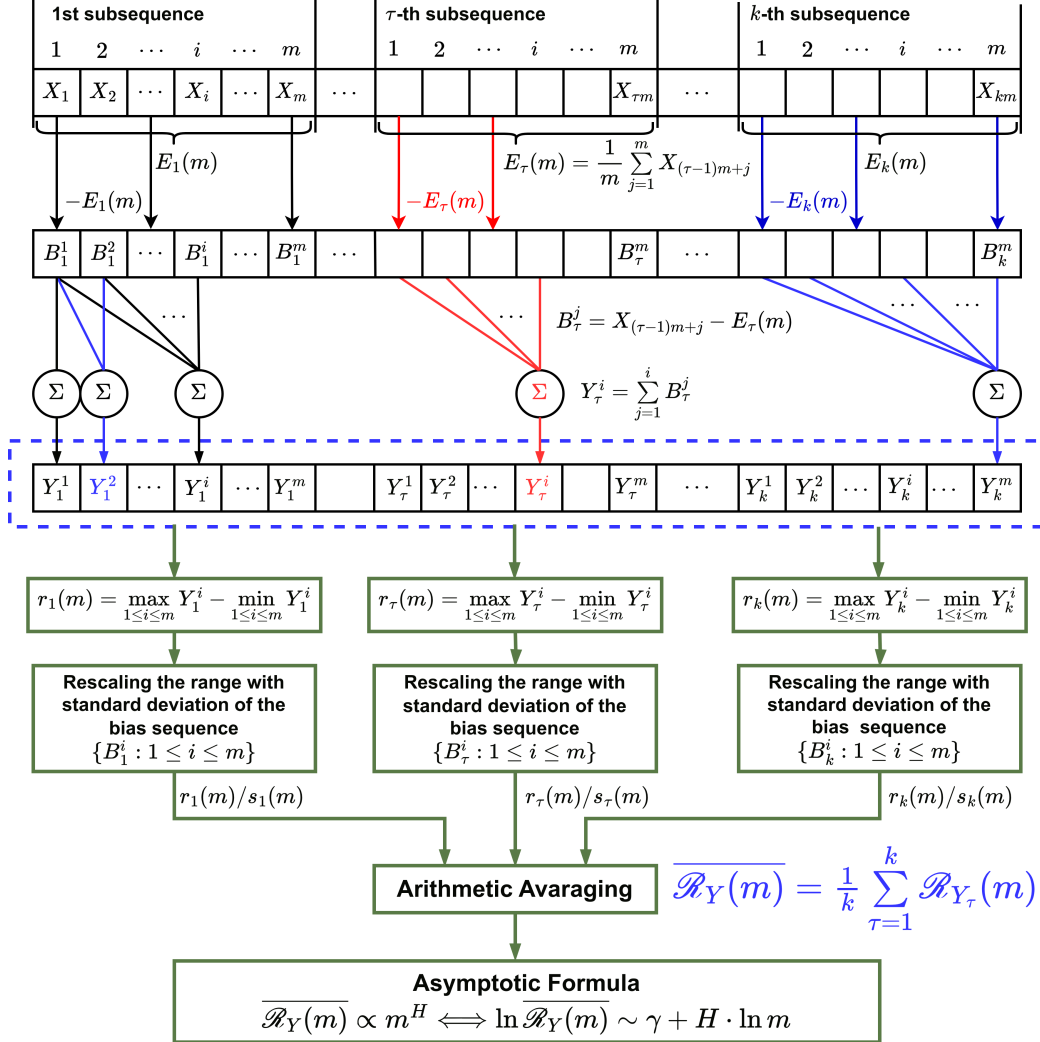


Figure 4: Partition of time sequence and structure of cumulative sequence for R/S analysis

Here we give some interpretations for the steps of the R/S estimator:

0) Pre-conditioning: Partitioning the sequence  $\{X_t : 1 \leq t \leq N\}$  into  $k$  subsequences with minimal size  $w$  such that  $N_{\text{opt}} = mk$  and  $m \in S_{\text{bpf}}(N_{\text{opt}}, w) = \{m_1, m_2, \dots, m_n\}$  where  $n = |S_{\text{bpf}}(N_{\text{opt}}, w)|$ .

i) For each subsequence, computing its local arithmetic average by

$$E_\tau(m) = \mathcal{A}_j^{1:m} \{X_{(\tau-1)m+j}\}. \quad (66)$$

ii) Construct the  $\tau$ -th local biased/detrended sequence

$$B_\tau = \{B_\tau^j : 1 \leq j \leq m\} \quad (67)$$

in which

$$B_\tau^j = X_{m(\tau-1)+j} - E_\tau(m), \quad 1 \leq j \leq m \quad (68)$$

and the cumulative bias sequence

$$Y_\tau = \{Y_\tau^i : 1 \leq i \leq m\} \quad (69)$$

where

$$Y_\tau^i = \mathcal{C}_j^{1:i} \{B_\tau^j\} = \sum_{j=1}^i B_\tau^j, \quad 1 \leq i \leq m. \quad (70)$$

iii) Calculating the unbiased standard deviation of the local bias sequence

$$s_\tau(m) = \mathcal{S}_j^{1:m} \{B_\tau^j\}, \quad 1 \leq \tau \leq k \quad (71)$$

iv) Calculating the range for the  $\tau$ -th cumulative bias sequence  $Y_\tau$

$$r_\tau(m) = \max_{1 \leq i \leq m} Y_\tau^i - \min_{1 \leq i \leq m} Y_\tau^i, \quad 1 \leq \tau \leq k \quad (72)$$

v) Computing the R/S statistics of the sequence  $Y_\tau$

$$\mathcal{R}_{Y_\tau}(m) = \frac{r_\tau(m)}{s_\tau(m)} \quad (73)$$

vi) Calculating the arithmetic average of each R/S statistics

$$\overline{\mathcal{R}_Y(m)} = \mathcal{A}_\tau^{1:k} \{\mathcal{R}_{Y_\tau}(m)\} = \frac{1}{k} \sum_{\tau=1}^k \frac{r_\tau(m)}{s_\tau(m)}. \quad (74)$$

in order to get the asymptotic relation

$$\overline{\mathcal{R}_Y(m)} \propto m^H \iff \ln \overline{\mathcal{R}_Y(m)} \sim \gamma + H \cdot \ln m$$

vii) Repeating the steps i)~v) for  $n$  times for different choices of  $m$  and setting

$$\begin{cases} \mathbf{T} = [m_1, \dots, m_n]^\top \\ \mathbf{S} = [S(m_1), \dots, S(m_n)]^\top \\ \langle \mathbf{A}, \mathbf{b} \rangle \leftarrow \text{FORMATPOWLAWDATA}(\mathbf{T}, \mathbf{S}, n) \end{cases}$$

viii) Estimating the Hurst exponent with linear regression

$$\mathbf{p}_{\text{RS}} \leftarrow \text{LINEARREGRSOLVER}(\mathbf{A}, \mathbf{b}, k, \text{flag})$$

where  $\mathbf{p}_{\text{RS}} = [\hat{\alpha}_{\text{RS}}, \hat{\beta}_{\text{RS}}]^\top$ , which implies that

$$\hat{H}_{\text{RS}} = \hat{\beta}_{\text{RS}}.$$

Particularly, the theoretical values of the R/S statistics of white noise are usually approximated by [53]

$$\mathbb{E} \{ \mathcal{R}_Y(m) \} = \begin{cases} \frac{m-\frac{1}{2}}{m} \cdot \frac{\Gamma(\frac{m-1}{2})}{\sqrt{\pi} \Gamma(\frac{m}{2})} \cdot \sum_{i=1}^{m-1} \sqrt{\frac{m-i}{i}}, & n \leq 340 \\ \frac{m-\frac{1}{2}}{m} \cdot \sqrt{\frac{2}{\pi m}} \cdot \sum_{i=1}^{m-1} \sqrt{\frac{m-i}{i}}, & n > 340 \end{cases} \quad (75)$$

where the  $\Gamma(x) = \int_0^{+\infty} t^{x-1} e^{-t} dt$  in (75) is the Gamma function and the factor  $(m-1/2)/m$  was added by Peters [54] to improve the accuracy for small  $m$ . Thus we can construct the revised R/S statistics [52]:

$$\mathcal{R}_Y^{\text{AL}}(m) = \mathcal{R}_Y(m) - \mathbb{E} \{ \mathcal{R}_Y(m) \} + \sqrt{\frac{\pi m}{2}} \quad (76)$$

for the  $Y_\tau$  which has the asymptotic behavior

$$\mathcal{R}_Y^{\text{AL}}(m) \propto m^H \iff \ln \mathcal{R}_Y^{\text{AL}}(m) \sim \gamma + H \cdot \ln m. \quad (77)$$

for (74). It should be noted that the estimation for the Hurst exponent via revised statistic  $\mathcal{R}_{Y_\tau}^{\text{AL}}$  will be smaller than the true value when  $H > 0.5$  if replacing the (74) with (76).

## 4.5.2 Algorithm for R/S Estimator

The **Algorithm 11**, which is designed according to (66), (67), (68), (69), (70), (71), (72), (73), (74) and (77), provides a procedure for calculating the Hurst exponent of a time sequence with the help of (77).

---

### Algorithm 11 Rescaled Range Analysis Estimator for Hurst exponent

---

**Input:** Time sequences data  $\mathbf{X}$ , window size  $w$ , indicator **flag** for the optimization method in linear regression.

**Output:** Hurst exponent of the sequence  $\mathbf{X}$ .

```

1: procedure ESTHURSTRS( $\mathbf{X}, w, \mathbf{flag}$ )
2:    $N \leftarrow \text{GETLENGTH}(\mathbf{X});$ 
3:    $N_{\text{opt}} \leftarrow \text{SEARCHOPTSEQLEN}(N, w);$ 
4:    $\mathbf{T} \leftarrow \text{GENSBPF}(N_{\text{opt}}, w);$ 
5:    $n \leftarrow \text{GETLENGTH}(\mathbf{T});$ 
6:    $\mathbf{S} \leftarrow \mathbf{0} \in \mathbb{R}^{n \times 1};$  // For the statistics
7:   for  $\text{idx} \in \langle 1, 2, \dots, n \rangle$  do
8:      $m \leftarrow T_{\text{idx}};$ 
9:      $k \leftarrow N_{\text{opt}}/m;$ 
10:     $\mathbf{L} \leftarrow \mathbf{0} \in \mathbb{R}^{n \times 1};$  // For the rescaled range
11:    for  $\tau \in \langle 1, 2, \dots, k \rangle$  do
12:       $E_{\tau} \leftarrow \mathcal{A}_i^{1:m} \{X_{(\tau-1)m+i}\};$ 
13:       $\mathbf{B}_{\tau} \leftarrow \mathbf{0} \in \mathbb{R}^{m \times 1};$ 
14:      for  $j \in \langle 1, 2, \dots, m \rangle$  do
15:         $B_{\tau}^j = X_{(\tau-1)m+j} - E_{\tau};$ 
16:      end for
17:       $\mathbf{Y}_{\tau} \leftarrow \mathbf{0} \in \mathbb{R}^{m \times 1};$ 
18:      for  $i \in \{1, \dots, m\}$  do
19:         $Y_{\tau}^i \leftarrow \mathcal{C}_j^{1:i} \{B_{\tau}^j\};$ 
20:      end for
21:       $r_{\tau}(m) \leftarrow \max_{1 \leq i \leq m} Y_{\tau}^i - \min_{1 \leq i \leq m} Y_{\tau}^i;$ 
22:       $s_{\tau}(m) \leftarrow \mathcal{S}_i^{1:m} \{B_{\tau}^i\};$ 
23:       $L_{\tau} \leftarrow r_{\tau}(m)/s_{\tau}(m);$ 
24:    end for
25:     $S_{\text{idx}} \leftarrow \mathcal{A}_{\tau}^{1:k} \{L_{\tau}\};$  // by (70)
26:  end for
27:   $\langle \mathbf{A}, \mathbf{b} \rangle \leftarrow \text{FORMATPOWLAWDATA}(\mathbf{T}, \mathbf{S}, n);$ 
28:   $\mathbf{p} \leftarrow \text{LINEARREGRSOLVER}(\mathbf{A}, \mathbf{b}, n, \mathbf{flag});$ 
29:   $\beta_{\text{RS}} \leftarrow p_2;$  //  $\mathbf{p} = [\alpha, \beta]^{\text{T}};$ 
30:   $H \leftarrow \beta_{\text{RS}};$ 
31:  return  $H;$ 
32: end procedure

```

---

## 4.6 Triangles Total Areas (TTA) Method

### 4.6.1 Principle of TTA Estimator

For time sequence  $\{X_t\}_{t=1}^N$ , we can derive the *triangles total areas* (TTA) method with the cumulative sequence

$$Y_i = \mathcal{C}_t^{1:i} \{X_t - \bar{X}\}, \quad 1 \leq i \leq n. \quad (78)$$

For the fixed time lag  $\tau \in \mathbb{N}$  and  $i$ -th group of vertices  $\{P_i, Q_i, R_i\} \subset \mathbb{R}^2$  such that

$$\begin{cases} P_i = (i, Y_i) \\ Q_i = (i + \tau, Y_{i+\tau}) \\ R_i = (i + 2\tau, Y_{i+2\tau}) \end{cases} \quad 1 \leq i \leq \lfloor \frac{N-1}{2\tau} \rfloor$$

for the triangle  $\Delta P_i Q_i R_i$ , its area can be calculated with the 3-order determinant, viz.

$$A_i = \frac{1}{2} \left| \det \begin{pmatrix} i & i + \tau & i + 2\tau \\ Y_i & Y_{i+\tau} & Y_{i+2\tau} \\ 1 & 1 & 1 \end{pmatrix} \right| = \frac{\tau}{2} |Y_{i+2\tau} - 2Y_{i+\tau} + Y_i|, \quad 1 \leq i \leq \lfloor \frac{N-1}{2\tau} \rfloor \quad (79)$$

then the total area of the triangles is

$$A_{\text{total}}(\tau) = \frac{\tau}{2} \sum_{j=1}^{\lfloor \frac{N-1}{2\tau} \rfloor} A_i. \quad (80)$$

**Figure 5** illustrates the relevant details of the construction for each triangle and the total area.

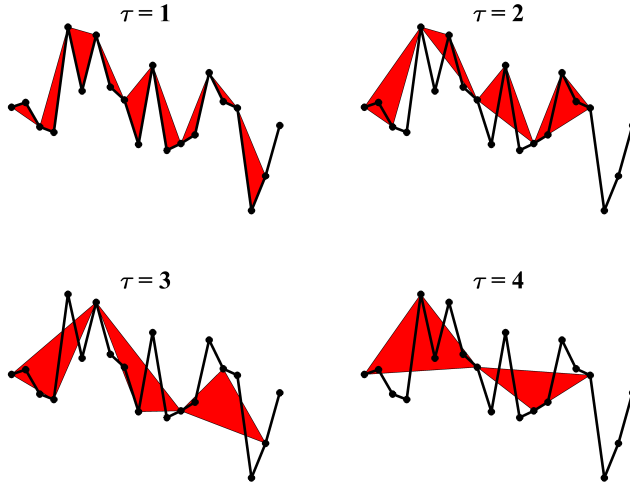


Figure 5: Construction of triangles with four different lags  $\tau = 1, 2, 3, 4$ .

Lotfalinezhad and Maleki [9] showed that

$$A_{\text{total}}(\tau) \propto \tau^H \iff \ln A_{\text{total}}(\tau) \sim \alpha_{\text{TTA}} + \beta_{\text{TTA}} \cdot \ln \tau \quad (81)$$

Consequently, we have

$$\hat{H}_{\text{TTA}} = \hat{\beta}_{\text{TTA}} \quad (82)$$

by linear regression. The *triangles areas method* (TA), a modification of the TTA method, proposed in [10] has similar principle, and the modification is just to consider the distribution of the area of the triangles instead of the distribution of the sum of the total areas of the triangles involved.

#### 4.6.2 Algorithm for TTA Estimator

With the help of (78), (79), (80), (81) and (82), we can design the estimation algorithm for the TTA method, please see **Algorithm** alg-TTA. Note that we set  $\tau_{\text{max}} = 10$  in **Algorithm** 12 as we have done in **Algorithm** 8.

---

**Algorithm 12** Total Triangle Area Method for Estimating Hurst Exponent

---

**Input:** Time series data  $\mathbf{X}$ , indicator **flag** for the optimization method in linear regression.

**Output:** Hurst exponent of the sequence  $\mathbf{X}$ .

```
1: procedure ESTHURSTTTA( $\mathbf{X}$ , flag)
2:    $n \leftarrow 10$ ; //  $\tau_{\max} = 10$ 
3:    $N \leftarrow \text{GETLENGTH}(\mathbf{X})$ ;
4:    $\mathbf{T} \leftarrow \langle 1, 2, \dots, n \rangle$ ;
5:    $\mathbf{S} \leftarrow \mathbf{0} \in \mathbb{R}^{n \times 1}$ ; // For the statistics
6:    $\bar{X} \leftarrow \mathcal{A}_i^{1:N} \{X_i\}$ ;
7:   for  $i \in \langle 1, 2, \dots, N \rangle$  do
8:      $Y_i \leftarrow \mathcal{C}_j^{1:i} \{X_j - \bar{X}\}$ ;
9:   end for
10:  for  $\text{idx} \in \langle 1, 2, \dots, n \rangle$  do
11:     $\text{sum} \leftarrow 0$ ;
12:    for  $i \in \langle 1, 2, \dots, \lfloor \frac{N-1}{2\tau} \rfloor \rangle$  do
13:       $j \leftarrow 2(i-1)\tau + 1$ ; // by (79)
14:       $\text{sum} \leftarrow \text{sum} + |Y_{j+2\tau} - 2Y_{j+\tau} + Y_j|$ ;
15:    end for
16:     $S_{\text{idx}} \leftarrow \text{idx} \cdot \text{sum}/2$ ;
17:  end for
18:   $\langle \mathbf{A}, \mathbf{b} \rangle \leftarrow \text{FORMATPOWLAWDATA}(\mathbf{T}, \mathbf{S}, n)$ ;
19:   $\mathbf{p} \leftarrow \text{LINEARREGRSOLVER}(\mathbf{A}, \mathbf{b}, n, \text{flag})$ ;
20:   $\beta_{\text{TTA}} \leftarrow p_2$ ; //  $\mathbf{p} = [\alpha, \beta]^T$ ;
21:   $H \leftarrow \beta_{\text{TTA}}$ ; // by (82)
22:  return  $H$ ;
23: end procedure
```

---

## 4.7 Periodogram Method (PM)

### 4.7.1 Principle of Periodogram Estimator

Geweke and Porter-Hudak [15] proposed the *periodogram method* (PM) for estimating the Hurst exponent. The periodogram for a time sequence  $\{X_t : 1 \leq t \leq N\}$  can be calculated by

$$I(k) = \frac{1}{N} \left| \sum_{t=1}^N X_t e^{-\frac{2\pi i}{N}(k-1)(t-1)} \right|^2, \quad 1 \leq k \leq N \quad (83)$$

where  $i = \sqrt{-1}$  and  $I(k)$  in (83) is the squared absolute value of the DFT of the sequence  $X_t$ . Weron et al. showed that [52]

$$I(k) \propto \left[ 4\sin^2 \left( \frac{k}{2N} \right) \right]^{\frac{1}{2}-H}, \quad 1 \leq k \leq \left\lfloor \frac{N}{2} \right\rfloor \quad (84)$$

or equivalently

$$\ln I(k) \sim \alpha_{\text{PM}} + \beta_{\text{PM}} \cdot \ln \left[ 4\sin^2 \left( \frac{k}{2N} \right) \right], \quad 1 \leq k \leq \left\lfloor \frac{N}{2} \right\rfloor. \quad (85)$$

In consequence, we have

$$\hat{H}_{\text{PM}} = \frac{1}{2} - \hat{\beta}_{\text{PM}} \quad (86)$$

by performing the linear regression for (85).

### 4.7.2 Algorithm for Periodogram Estimator

It should be noted that the spectrum-domain method relies more advanced mathematical concepts and tools. In the **Algorithm 13** based on (83), (84), (85) and (86), we can take the procedure FFT to transform a time sequence into spectrum-domain. Since there are lots of toolboxes for the FFT in C/C++/MATLAB/Python/R, the details for the principle and algorithm implementation are omitted here.

---

#### Algorithm 13 Periodogram Estimator for Hurst exponent

---

**Input:** Time sequence  $\mathbf{X}$ , the cut-off frequency  $f_{\text{cutoff}}$ , indicator **flag** for the optimization method in linear regression.

**Output:** Hurst exponent of the sequence  $\mathbf{X}$ .

```

1: procedure ESTHURSTPERIODDIAGRAM( $\mathbf{X}$ ,  $f_{\text{cutoff}}$ , flag)
2:    $N \leftarrow \text{GETLENGTH}(\mathbf{X})$ ;
3:    $\mathbf{Y} \leftarrow \text{FFT}(\mathbf{X})$ ;
4:    $\mathbf{T} \leftarrow \emptyset$ ; //  $\mathbf{T}$  is used for the  $4 \sin^2(k/(2N))$ , according to (84)
5:    $\mathbf{S} \leftarrow \emptyset$ ; //  $\mathbf{S}$  is used for the periodogram  $I(k)$ , according to (83)
6:   for  $k \in \langle 2, \dots, \lfloor \frac{N}{2} \rfloor \rangle$  do // Attention, please!
7:      $f \leftarrow k/N$ ; // Calculate frequencies
8:     if  $f \leq f_{\text{cutoff}}$  then
9:        $\mathbf{T} \leftarrow \mathbf{T} \cup \{4 \sin^2(f/2)\}$ ;
10:       $\mathbf{S} \leftarrow \mathbf{S} \cup \{|Y_k|^2 / N\}$ ;
11:     end if
12:   end for
13:    $n \leftarrow \text{GETLENGTH}(\mathbf{T})$ ;
14:    $\langle \mathbf{A}, \mathbf{b} \rangle \leftarrow \text{FORMATPOWLAWDATA}(\mathbf{T}, \mathbf{S}, n)$ ;
15:    $\mathbf{p} \leftarrow \text{LINEARREGRSOLVER}(\mathbf{A}, \mathbf{b}, n, \mathbf{flag})$ ;
16:    $\beta_{\text{PD}} \leftarrow p_2$ ; //  $\mathbf{p} = [\alpha, \beta]^T$ ;
17:    $H \leftarrow 0.5 - \beta_{\text{PD}}$ ; // by (86)
18:   return  $H$ ;
19: end procedure

```

---

## 4.8 Discrete Wavelet Transform (DWT) Method

It is also feasible to estimate the Hurst exponent with discrete wavelet transform. The time sequence  $\mathbf{X} = \{X_t\}_{t=1}^N$  can be transformed into the spectrum-domain by

$$W_{\mathbf{X}}(a, b) = \text{DWT}_b^a(\mathbf{X}, \psi)$$

where  $a$  is the scale parameter,  $b$  is the location parameter,  $\psi$  is the wavelet function and  $\text{DWT}_b^a$  is the DWT for the details of the time sequence according to (19). For the given scale  $a$ , we can find a representation of the wavelet “energy” or amplitude and study its scaling for exploring the power law of interest when estimating the Hurst exponent [55].

### 4.8.1 Average Wavelet Coefficient Method (AWC)

The *average wavelet coefficient* (AWC) method is based on the self-affine correlations of the DWT of a time sequence, which can be used for estimating the Hurst exponent. Simonsen [21] showed that

$$W_{\mathbf{X}}^{\text{awc}}(a) = \frac{1}{|I_a|} \sum_{b \in I_a} |W(a, b)| \sim a^{H-0.5} \quad (87)$$

where  $I_a$  is defined by (16). Taking the logarithms of both sides in (87), we immediately have

$$\ln W_{\mathbf{X}}^{\text{awc}}(a) \sim \alpha_{\text{AWC}} + \beta_{\text{AWC}} \cdot \ln a. \quad (88)$$

Consequently, we can obtain

$$\hat{H}_{\text{AWC}} = \hat{\beta}_{\text{AWC}} + \frac{1}{2} \quad (89)$$

by (88) with the help of linear regression.

#### 4.8.2 Variance Versus Level (VVL) Method

Similar to the AWC method, we can construct the *variance versus level* VVL spectrum over all of the location parameters  $b \in I_a$  for the given scale  $a$ . Let

$$W_{\mathbf{X}}^{\text{vvl}}(a) = \frac{1}{|I_a| - 1} \sum_{b \in I_a} [|W(a, b)| - W_{\mathbf{X}}^{\text{awc}}(a)]^2 \quad (90)$$

be the variance of  $|W(a, b)|$  respect to the discrete location variable  $b$ . Flandrin [20] discovered the asymptotic formula

$$W_{\mathbf{X}}^{\text{vvl}}(a) \sim a^{2H-1} \quad (91)$$

for (90). Equivalently, we have

$$\ln W_{\mathbf{X}}^{\text{vvl}}(a) \sim \alpha_{\text{VVL}} + \beta_{\text{VVL}} \cdot \ln a \quad (92)$$

by taking the logarithm on the both sides of (91). In consequence, the new estimator of Hurst exponent can be written by

$$\hat{H}_{\text{VVL}} = (1 + \hat{\beta}_{\text{VVL}})/2. \quad (93)$$

#### 4.8.3 Algorithm for DWT Estimator

It is easy to find there is a unified formula for the AWC and VVL methods. Combining (89) and (93), we have

$$\hat{H}_{\text{DWT}} = \frac{1}{2} + \frac{\hat{\beta}_{\text{DWT}}}{r} = \begin{cases} 0.5 + \hat{\beta}_{\text{AWC}} & r = 1 \\ 0.5 + 0.5 \cdot \hat{\beta}_{\text{VVL}}, & r = 2 \end{cases} \quad (94)$$

Thus it is convenient for us to design a unified interface for estimating the Hurst exponent with the AWC method and the VVL method.

The **Algorithm 14** is designed according to (90), (91), (92),(93) and (94) with the help of DWT. Currently, the DWT algorithm is a built-in function in MATLAB, Python and R. We remark that here we take a unified interface WAVEDEC to achieve the multilevel DWT for 1-dim time sequences.

---

#### **Algorithm 14** Discrete Wavelet Transform Estimator for Hurst exponent

---

**Input:** Time sequences data  $\mathbf{X}$ , integer  $r \in \langle 1, 2 \rangle$  for the AWC/VVL method, indicator **flag** for the optimization method in linear regression.

**Output:** Hurst exponent of the sequence  $\mathbf{X}$ .

```

1: procedure ESTHURSTDWT( $\mathbf{X}$ ,  $r$ , flag)
2:    $N \leftarrow \text{GETLENGTH}(\mathbf{X});$ 
3:    $n \leftarrow \lfloor \log_2(N) \rfloor;$  // Calculate appropriate decomposition level
4:   if  $r = 1$  then
5:      $\mathbf{W} \leftarrow \text{WAVEDEC}(\mathbf{X}, \text{"db24"}, n);$  // 24-th order Daubechies DWT
6:   else
7:      $\mathbf{W} \leftarrow \text{WAVEDEC}(\mathbf{X}, \text{"haar"}, n);$  // Haar DWT
8:   end if
9:    $\mathbf{T} \leftarrow \mathbf{0} \in \mathbb{R}^{n \times 1};$  // For the scale
10:   $\mathbf{S} \leftarrow \mathbf{0} \in \mathbb{R}^{n \times 1};$  // For the AWC-spectrum
11:  for  $\text{idx} \in \langle 1, 2, \dots, n \rangle$  do
12:     $T_{\text{idx}} \leftarrow 2^{\text{idx}};$  // Add scale coefficient

```

```

13:    $\mathbf{L}_{\text{pos}} \leftarrow |W_{\text{idx}}|$ ; // All location parameters corresponding to scale  $2^{\text{idx}}$ 
14:   if  $r = 1$  then
15:      $S_{\text{idx}} \leftarrow \text{MEAN}(\mathbf{L}_{\text{pos}})$ ; // AWC-spectrum, by (87)
16:   else
17:      $S_{\text{idx}} \leftarrow \text{Var}(\mathbf{L}_{\text{pos}})$ ; // VVL-spectrum, by (90)
18:   end if
19: end for
20:  $\langle \mathbf{A}, \mathbf{b} \rangle \leftarrow \text{FORMATPOWLAWDATA}(\mathbf{T}, \mathbf{S}, n)$ ;
21:  $\mathbf{p} \leftarrow \text{LINEARREGRSOLVER}(\mathbf{A}, \mathbf{b}, n, \text{flag})$ ;
22:  $\beta_{\text{DWT}} \leftarrow p_2$ ; //  $\mathbf{p} = [\alpha, \beta]^T$ ;
23:  $H \leftarrow \beta_{\text{DWT}}/r + 0.5$ ; // by (94)
24: return  $H$ ;
25: end procedure

```

---

## 4.9 Local Whittle (LW) Method

### 4.9.1 Principle of LW Estimator

As the similar process stated in the PM method, for the vector  $\boldsymbol{\lambda} = [\lambda_1, \dots, \lambda_n]^T$  such that  $\lambda_j = \frac{2\pi j}{N}$  for  $j \in \{1, 2, \dots, n = \lfloor \frac{N}{2} \rfloor\}$ , we set

$$\mathbf{I}(\boldsymbol{\lambda}) = [I_1, \dots, I_n]^T = \left[ |\omega(\lambda_1)|^2, \dots, |\omega(\lambda_n)|^2 \right]^T \quad (95)$$

where

$$\omega(\lambda_j) = \frac{1}{N} \sum_{t=1}^N X_t e^{i(t-1)\lambda_j} \quad (96)$$

is the DFT of the TS  $X_t = \{X_1, \dots, X_N\}$ . Kunsch et al [16] showed that the Hurst exponent can be estimated by solving the following optimization problem

$$\hat{H}_{\text{LW}} = \arg \min_{H \in (0,1)} \psi(H) \quad (97)$$

with the objective function

$$\psi(H) = \ln \left[ \frac{1}{n} \sum_{j=1}^n \lambda_j^{2H-1} I_j \right] - \frac{2H-1}{n} \sum_{j=1}^n \ln \lambda_j \quad (98)$$

where the  $j$ -th component  $I_j$  is defined by (95). For more details, please see Robinson's work [17].

### 4.9.2 Algorithm for LW Estimator

The procedure ESTHURSTLW listed in **Algorithm 15** is designed for estimating the Hurst exponent with the LW method specified by (95), (96), (97) and (98). We remarked that there are two procedures that are involved in **Algorithm 15**:

- the procedure OBJFUNLW is used to compute the value of  $\psi(H)$  determined by (98), and
- the procedure LOCMINSOLVER to find the minimum of  $\psi(H)$ , please see the **Algorithm 24** in the Appendix A for more details.

---

**Algorithm 15** Estimating the Hurst exponent with the Local Whittle method

---

**Input:** Time sequence  $\mathbf{X}$ .

**Output:** Hurst exponent of the sequence  $\mathbf{X}$ .

1: **procedure** ESTHURSTLW( $\mathbf{X}$ )

```

2:   $N \leftarrow \text{GETLENGTH}(\mathbf{X});$  // Length of the original sequence
3:   $\mathbf{Y} \leftarrow \text{FFT}(\mathbf{X});$ 
4:   $n \leftarrow \lfloor N/2 \rfloor;$ 
5:   $\mathbf{T} \leftarrow \mathbf{0} \in \mathbb{R}^{n \times 1};$  // for the frequencies
6:   $\mathbf{S} \leftarrow \mathbf{0} \in \mathbb{R}^{n \times 1};$  // for the periodogram
7:  for  $\text{idx} \in \langle 1, \dots, n \rangle$  do // Attention, please!
8:       $T_{\text{idx}} \leftarrow \text{idx}/N;$  // Calculate frequencies
9:       $S_{\text{idx}} \leftarrow |Y_{\text{idx}+1}|^2;$  // Periodogram, see (95)
10: end for
11:  $H \leftarrow \text{LOCMIN SOLVER}(\text{OBJFUNLW}, [0.001, 0.999], 10^{-8}, \langle \mathbf{T}, \mathbf{S} \rangle);$  // by (97)
12: return  $H;$ 
13: end procedure

```

---

**Algorithm 16** Computing the objective function  $\psi(H)$  in Local Whittle method

---

**Input:** Variable  $H \in (0, 1)$ , frequency vector  $\mathbf{T}$  and periodogram vector  $\mathbf{S}$ .

**Output:**  $\psi(H)$ .

```

1: procedure OBJFUNLW( $x, \langle \mathbf{T}, \mathbf{S} \rangle$ )
2:    $n \leftarrow \text{GETLENGTH}(\mathbf{T});$  //  $n = \lfloor N/2 \rfloor$ 
3:    $y \leftarrow \ln \left( \frac{1}{n} \sum_{i=1}^n T_i^{2H-1} S_i \right) - \frac{2H-1}{n} \sum_{i=1}^n \ln T_i;$ 
4:   return  $y;$  // by (98)
5: end procedure

```

---

## 4.10 Least Squares via Standard Deviation (LSSD)

### 4.10.1 Principle of LSSD Estimator

The Hurst exponent can also be estimated with the *least squares via standard deviation* (LSSD). The steps are summarized as follows:

- 0) Pre-conditioning: Dividing the sequence  $\{X_t\}_{t=1}^N$  into  $k = \lfloor N/m \rfloor$  subsequences with the same size  $m$  according to (35) where  $m \in \{1, 2, \dots, m_{\max}\}$  such that  $m_{\max} \geq \lfloor \frac{N}{10} \rfloor$  and each  $m$  corresponds to a partition scheme.
- i) Calculating the cumulative sum of the  $i$ -th subsequence  $X_{(i)} = \{X_{(i-1)m+j} : 1 \leq j \leq m\}$ , viz.

$$Z_i^m = \mathcal{C}_j^{1:m} \{X_{(i-1)m+j}\}, \quad 1 \leq i \leq \left\lfloor \frac{N}{m} \right\rfloor \quad (99)$$

- ii) Creating the standard deviation sequences  $\{s_m\}_{m=1}^{m_{\max}}$  by

$$s_m = \mathcal{S}_i^{1:m} \{Z_i^m\}, \quad 1 \leq m \leq m_{\max} \quad (100)$$

Suppose

$$\mathbb{E} \{\overline{s_m}\} = \mathbb{E} \{\mathcal{A}_m^{1:m_{\max}} \{s_m\}\} = \sigma,$$

then the self-similarity property of the sequence implies that [12]

$$\mathbb{E} \{s_m\} \approx \sigma \cdot c_{\text{LSSD}}(m, H) \cdot m^H$$

where  $H$  is the Hurst exponent and

$$c_{\text{LSSD}}(m, H) = \sqrt{\frac{N/m - (N/m)^{2H-1}}{N/m - 1/2}}. \quad (101)$$

iii) Constructing the optimization problem. Koutsoyiannis et al. [56] introduced the following function for fitting error

$$\mathcal{E}_{\text{LSSD}}^2(\sigma, H) = \sum_{m=1}^{m_{\max}} \frac{\left[ \ln \frac{\mathbb{E}\{s_m\}}{s_m} \right]^2}{m^p} + \frac{H^{q+1}}{q+1} = \sum_{m=1}^{m_{\max}} \frac{[\ln \sigma + H \cdot \ln m + \ln c_{\text{LSSD}}(m, H) - \ln s_m]^2}{m^p} + \frac{H^{q+1}}{q+1} \quad (102)$$

where  $p \in \{0, 1, 2, \dots\}$  is a weight parameter and  $H^{q+1}/(q+1)$  is a penalty factor with default value  $q = 50$ .

With the help of the least squares approach, we can solve (102) to obtain a fixed-point equation for the Hurst exponent, which can be written by

$$H = \Phi_{\text{LSSD}}(H) \quad (103)$$

in which

$$\begin{cases} \Phi_{\text{LSSD}}(H) = \frac{a_{11}[b_2(H) - H^q] - a_{21}(H)b_1(H)}{a_{11}a_{22}(H) - a_{21}(H)a_{12}}, \\ d_m(H) = \ln m + \frac{\ln(N/m)}{1 - (N/m)^{2-2H}}, \\ a_{11} = \sum_{m=1}^{m_{\max}} \frac{1}{m^p}, \quad a_{12} = \sum_{m=1}^{m_{\max}} \frac{\ln m}{m^p}, \quad a_{21}(H) = \sum_{m=1}^{m_{\max}} \frac{d_m(H)}{m^p}, \quad a_{22}(H) = \sum_{m=1}^{m_{\max}} \frac{d_m(H) \ln m}{m^p}, \\ b_1(H) = \sum_{m=1}^{m_{\max}} \frac{[\ln s_m - \ln c_{\text{LSSD}}(m, H)]}{m^p}, \quad b_2(H) = \sum_{m=1}^{m_{\max}} \frac{d_m(H) [\ln s_m - \ln c_{\text{LSSD}}(m, H)]}{m^p}. \end{cases} \quad (104)$$

Obviously, we can use the Newton's iterative method or direct iterative method to solve the fixed-point in order to estimate the exponent. Koutsoyiannis et al. [56] pointed out that there is a unique fixed-point for the equation (103), which can be solved with **Algorithm 3**. For more details of fixed-point algorithm, please see Zhang et al. [47] or the toolbox of MATLAB, Python, and so on.

#### 4.10.2 Algorithm for LSSD Estimator

The procedure ESTHURSTLSSD listed in **Algorithm 17** is designed to estimate the Hurst exponent with the LSSD method based on (99), (100), (101), (102), (103) and (104). Note that the procedure CTMLSSD is used to compute the contractive mapping  $\Phi_{\text{LSSD}}(H)$  and the procedure FIXED-POINTSOLVER listed in **Algorithm 3** provides a general interface for solving the fixed-point of some nonlinear equation.

---

#### Algorithm 17 LSSD Estimator

---

**Input:** Time sequence  $\mathbf{X}$ , weight  $p$ , penalty parameter  $q$ , precision  $\epsilon$  with default value  $\epsilon = 10^{-4}$ .

**Output:** Hurst exponent of the sequence  $\mathbf{X}$ .

- 1: **procedure** ESTHURSTLSSD( $\mathbf{X}, p, q, \epsilon$ )
- 2:      $N \leftarrow \text{GETLENGTH}(\mathbf{X});$
- 3:      $m_{\max} \leftarrow \lfloor N/10 \rfloor;$
- 4:      $\mathbf{T} \leftarrow \langle 1, 2, \dots, m_{\max} \rangle;$
- 5:      $\mathbf{S} \leftarrow \mathbf{0} \in \mathbb{R}^{m_{\max} \times 1};$  // For the standard deviation
- 6:     **for**  $\text{idx} \in \langle 1, 2, \dots, m_{\max} \rangle$  **do**
- 7:          $m \leftarrow \text{idx};$
- 8:          $k \leftarrow \lfloor N/m \rfloor;$
- 9:          $\mathbf{Z} \leftarrow \mathbf{0} \in \mathbb{R}^{k \times 1};$
- 10:        **for**  $i \in \langle 1, 2, \dots, k \rangle$  **do**

```

11:          $Z_i \leftarrow \sum_{j=1}^m X_{(i-1)m+j};$  // compute  $Z_i^m$  by (99)
12:     end for
13:      $S_{\text{idx}} \leftarrow \mathcal{S}_i^{1:k} \{Z_i\};$ 
14: end for
15:  $H \leftarrow \text{FIXEDPOINTSOLVER}(\text{CTMLSSD}, 0.5, \epsilon, N, p, q, \mathbf{T}, \mathbf{S});$  // by (103)
16: return  $H$ ;
17: end procedure

```

---

Please note that the Line 11 in **Algorithm 17** is based on (99). The procedures **FUNCMLSSD** listed in **Algorithm 18** and **FUNDMH** listed in **Algorithm 19** are used to compute the  $c_{\text{LSSD}}(m, H)$  and  $d_m(H)$  respectively. Furthermore, the procedure **CTMLSSD** for computing the  $\Phi_{\text{LSSD}}(H)$  listed in **Algorithm 20** is an argument of high order procedure **FIXEDPOINTSOLVER**.

---

**Algorithm 18** Computing the  $c_{\text{LSSD}}(m, H)$

---

**Input:** Positive integer  $m \in \{1, 2, \dots, m_{\max}\}$ , parameter  $H \in (0, 1)$ , Positive integer  $N$

**Output:** The value of  $c_{\text{LSSD}}(m, H)$

```

1: procedure FUNCMLSSD( $m, N, H$ )
2:      $u \leftarrow N/m;$ 
3:      $c \leftarrow \sqrt{(u - u^{2H-1})/(u - 0.5)};$  // by (101)
4:     return  $c$ ;
5: end procedure

```

---



---

**Algorithm 19** Computing the  $d_m(H)$

---

**Input:** Positive integer  $m \in \{1, 2, \dots, m_{\max}\}$ , parameter  $H \in (0, 1)$ , Positive integer  $N$

**Output:** The value of  $d_m(H)$

```

1: procedure FUNDMH( $m, N, H$ )
2:      $u \leftarrow N/m;$ 
3:      $d \leftarrow \ln m + \ln u / (1 - u^{2-2H});$ 
4:     return  $d$ ;
5: end procedure

```

---



---

**Algorithm 20** Contractive Mapping for the LSSD method

---

**Input:** Parameter  $H \in (0, 1)$ , length  $N$ , weight  $p$ , penalty parameter  $q$ , scale vector  $\mathbf{T} = [1, 2, \dots, m_{\max}]^T$ , standard deviation vector  $\mathbf{S} = [s_1, s_2, \dots, s_{m_{\max}}]^T$ .

**Output:** The value of  $\Phi_{\text{LSSD}}(H)$ .

```

1: procedure CTMLSSD( $H, \langle N, p, q, \mathbf{T}, \mathbf{S} \rangle$ )
2:      $m_{\max} \leftarrow \text{GETLENGTH}(\mathbf{T});$ 
3:      $a_{11} \leftarrow 0, a_{12} \leftarrow 0;$ 
4:      $a_{21} \leftarrow 0, a_{22} \leftarrow 0;$ 
5:      $b_1 \leftarrow 0, b_2 \leftarrow 0;$ 
6:     for  $\text{idx} \in \langle 1, 2, \dots, m_{\max} \rangle$  do
7:          $m \leftarrow T_{\text{idx}};$ 
8:          $s_m \leftarrow S_{\text{idx}};$ 
9:          $c_m \leftarrow \text{FUNCMLSSD}(m, N, H);$ 
10:         $d_m \leftarrow \text{FUNDMH}(m, N, H);$ 
11:         $u \leftarrow m^p;$ 
12:         $a_{11} \leftarrow a_{11} + 1.0/u;$  // by (104)
13:         $a_{12} \leftarrow a_{12} + \ln m/u;$ 

```

```

14:      $a_{21} \leftarrow a_{21} + d_m/u;$ 
15:      $a_{22} \leftarrow a_{22} + d_m \cdot \ln m/u;$ 
16:      $b_1 \leftarrow b_1 + (\ln s_m - \ln c_m)/u;$ 
17:      $b_2 \leftarrow b_2 + d_m \cdot (\ln s_m - \ln c_m)/u;$ 
18:   end for
19:    $g \leftarrow \frac{a_{11} \cdot (b_2 - H^q) - a_{21} \cdot b_1}{a_{11} \cdot a_{22} - a_{21} \cdot a_{12}};$  // by (104)
20:   return  $g;$ 
21: end procedure

```

---

## 4.11 Least Squares via Variance (LSV)

### 4.11.1 Principle of LSV Estimator

Similar to the LSSD-method, we can construct the variance sequences according to (99):

$$s_m^2 = (\mathcal{S}_i^{1:m} \{Z_i^m\})^2, \quad 1 \leq m \leq m_{\max}$$

The self-similarity property implies that

$$\mathbb{E} \{s_m^2\} = c_{\text{LSV}}(m, H) \cdot m^{2H} \cdot \sigma^2$$

where

$$c_{\text{LSV}}(m, H) = \frac{N/m - (N/m)^{2H-1}}{N/m - 1} \quad (105)$$

Tyralis et al. [11] introduced the fitting error function

$$\mathcal{E}_{\text{LSV}}^2(\sigma, H) = \sum_{k=1}^{k_{\max}} \frac{[c_{\text{LSV}}(m, H)k^{2H}\sigma^2 - s_m^2]^2}{m^p} + \frac{H^{q+1}}{q+1} \quad (106)$$

where  $p \in \{0, 1, 2, \dots\}$  is a weight parameter and  $H^{q+1}/(q+1)$  is a penalty factor with default value  $q = 50$ . By solving (106) with the least squares approach, Tyralis et al. [11] showed that the Hurst exponent can be estimated by solving the following optimization problem

$$\hat{H}_{\text{LSV}} = \arg \min_{H \in (0,1)} \Phi_{\text{LSV}}(H) \quad (107)$$

where

$$\Phi_{\text{LSV}}(H) = \sum_{m=1}^{m_{\max}} \frac{s_m^4}{m^p} - \frac{a_{12}^2(H)}{a_{11}(H)} + \frac{H^{q+1}}{q+1} \quad (108)$$

in which

$$\begin{cases} a_{11}(H) = \sum_{m=1}^{m_{\max}} \frac{[c_{\text{LSV}}(m, H)]^2 \cdot m^{4H}}{m^p} \\ a_{12}(H) = \sum_{m=1}^{m_{\max}} \frac{c_{\text{LSV}}(m, H) \cdot m^{2H} \cdot s_m^2}{m^p} \end{cases} \quad (109)$$

### 4.11.2 Algorithm for LSV Estimator

The procedure ESTHURSTLSV listed in **Algorithm 21** is designed for estimating the Hurst exponent with the LSV method. For the high order procedure LOCMINSOLVER involved in ESTHURSTLSV, please see **Algorithm 24**. Note that the procedure OBJFUNLSV, the first argument of LOCMINSOLVER, is given in **Algorithm 23**.

---

**Algorithm 21** Estimating the Hurst exponent with the LSV method

---

**Input:** Time sequence  $\mathbf{X}$ , weight  $p \in \{0, 1, 2, \dots\}$ , penalty parameter  $q \in \mathbb{N}$  with default value  $q = 50$ , precision  $\epsilon$  with default value  $\epsilon = 10^{-4}$ .

**Output:** Hurst exponent of the sequence  $\mathbf{X}$ .

```

1: procedure ESTHURSTLSV( $\mathbf{X}, p, q, \epsilon$ )
2:    $N \leftarrow \text{GETLENGTH}(\mathbf{X});$ 
3:    $m_{\max} \leftarrow \lfloor N/10 \rfloor;$ 
4:    $\mathbf{T} \leftarrow \langle 1, 2, \dots, m_{\max} \rangle;$ 
5:    $\mathbf{S} \leftarrow \mathbf{0} \in \mathbb{R}^{m_{\max} \times 1};$  // For the standard deviation
6:   for  $\text{idx} \in \langle 1, 2, \dots, m_{\max} \rangle$  do
7:      $m \leftarrow \text{idx};$  // size of the subsequences
8:      $k \leftarrow \lfloor N/m \rfloor;$  // number of subsequences
9:      $\mathbf{Z} \leftarrow \mathbf{0} \in \mathbb{R}^{k \times 1};$ 
10:    for  $i \in \langle 1, 2, \dots, k \rangle$  do
11:       $Z_i \leftarrow \sum_{j=1}^m X_{(i-1)m+j};$ 
12:    end for
13:     $S_{\text{idx}} \leftarrow \mathcal{S}_i^{1:m} \{Z_i\};$ 
14:  end for
15:   $H \leftarrow \text{LOCMINSOLVER}(\text{OBJFUNLSV}, [0.001, 0.999], \epsilon, N, p, q, \mathbf{T}, \mathbf{S});$  // by (107)
16:  return  $H;$ 
17: end procedure

```

The procedures FUNCMLSV listed in **Algorithm 22** is used to compute the  $c_{\text{LSV}}(m, H)$  according to (105). Note that the (107) are used to compute the fixed-point for the Hurst exponent.

---

**Algorithm 22** Computing the  $c_{\text{LSV}}(m, H)$

---

**Input:** Positive integer  $m \in \{1, 2, \dots, m_{\max}\}$ , parameter  $H \in (0, 1)$ , Positive integer  $N$

**Output:** The value of  $c_{\text{LSV}}(m, H)$

```

1: procedure FUNCMLSV( $m, N, H$ )
2:    $u \leftarrow N/m;$ 
3:    $c \leftarrow (u - u^{2H-1})/(u - 1);$  // by (105)
4:   return  $c;$ 
5: end procedure

```

The procedure OBJFUNLSV is used to compute the objective function  $\Phi_{\text{LSV}}(H)$  in (108) and (109) for estimating the Hurst exponent.

---

**Algorithm 23** Objective function  $\Phi_{\text{LSV}}(H)$  for the LSV method

---

**Input:** Hurst exponent  $H$ , length  $N$ , weight  $p$ , penalty parameter  $q$ , scale vector  $\mathbf{T} = [1, 2, \dots, m_{\max}]^{\top}$  and standard deviation vector  $\mathbf{S} = [s_1, s_2, \dots, s_{m_{\max}}]^{\top}$ .

**Output:** The value of  $\Phi_{\text{LSV}}(H)$  for the LSV method

```

1: procedure OBJFUNLSV( $H, N, p, q, \mathbf{T}, \mathbf{S}$ )
2:    $m_{\max} \leftarrow \text{GETLENGTH}(\mathbf{T});$ 
3:    $b_2 \leftarrow \frac{H^{q+1}}{q+1};$ 
4:    $a_{11} \leftarrow 0, a_{12} \leftarrow 0, b_1 \leftarrow 0;$ 
5:   for  $\text{idx} \in \{1, 2, \dots, m_{\max}\}$  do
6:      $m \leftarrow T_{\text{idx}};$ 
7:      $s_m \leftarrow S_{\text{idx}};$ 
8:      $c_m \leftarrow \text{FUNCMLSV}(m, N, H);$ 
9:      $u \leftarrow m^p;$ 

```

```

10:       $b_1 \leftarrow b_1 + s_m^4/u;$  // by (109)
11:       $a_{11} \leftarrow a_{11} + c_m^2 \cdot m^{4H}/u;$ 
12:       $a_{12} \leftarrow a_{12} + c_m \cdot m^{2H} \cdot s_m^2/u;$ 
13:  end for
14:   $g \leftarrow b_1 - \frac{a_{12} \cdot a_{12}}{a_{11}} + b_2;$  // by (108)
15:  return  $g;$ 
16: end procedure

```

---

## 5 Performance Assessment for the Typical Algorithms

### 5.1 Experimental Setup

Our experimental setup has the following configuration: Operating system — Ubuntu 22.04.3 LTS GNU/Linux(64-bit); Memory — 32GB RAM; Processor — 12th Gen Intel<sup>®</sup> Cor<sup>™</sup> i7-12700KF × 20; Programming language — Python 3.10.12.

### 5.2 Random Sequence and Hurst Exponent

For the short-correlated random sequences, their Hurst exponents fluctuate around the constant 0.5 [49]. We performed experiments with six types random distributions, including normal distribution  $\mathcal{N}(0, 1)$ , Chi-square distribution  $\chi^2(1)$ , geometric distribution  $\text{GE}(0.25)$ , Poisson distribution  $\mathcal{P}(5)$ , exponential distribution  $\text{Exp}(1)$ , and uniform distribution  $\mathcal{U}(0, 1)$ , to assess the performance of our algorithms when the sample sequences are random. For each distribution, we generated  $n = 30$  sets of sample sequences with a length of  $N = 10^4$  using the built-in random number generators in Python. Formally, the data set for the verification and validation is

$$\left\{ X_j^{(\star, i)} : 1 \leq j \leq 10^4 \right\}, \quad 1 \leq i \leq n$$

where  $\star \in \{\mathcal{N}(0, 1), \chi^2(1), \text{GE}(0.25), \mathcal{P}(5), \text{Exp}(1), \mathcal{U}(0, 1)\}$  denotes the type of distribution. Let  $\hat{H}_{\diamond}^{(\star, i)}$  be the Hurst exponent estimated from the  $i$ -th sample sequence  $\left\{ X_j^{(\star, i)} : 1 \leq j \leq 10^4 \right\}$  with the estimation method labeled by  $\diamond$ , then we have the arithmetic average

$$\overline{\hat{H}_{\diamond}^{\star}} = \frac{1}{n} \sum_{i=1}^n \hat{H}_{\diamond}^{(\star, i)}$$

where  $\diamond \in \{\text{AM}, \text{AV}, \text{GHE}, \text{HM}, \text{DFA}, \text{RS}, \text{TTA}, \text{PM}, \dots, \text{LSSD}, \text{LSV}\}$  denotes the estimation method.

For  $n = 30$  times repetitive experiments, the values of  $\overline{\hat{H}_{\diamond}^{\star}}$  are shown in **Table 3** for the short-correlated random sequences. Note that we set the window size  $w = 50$  for calculating the optimal length  $N_{\text{opt}}$  and  $\text{flag} = 2$  for the minimum  $\ell_2$ -norm method in linear regression. Obviously, the Hurst exponents estimated with the thirteen algorithms mentioned above fluctuates in the range  $0.45 \sim 0.55$ , which coincides with the conclusion presented of by Chen et al [49].

### 5.3 Estimation with Fractional Gaussian Noise Sequence

For the purpose of testing the accuracy of the algorithms for estimating the Hurst exponent of TS, we constructed multiple sets of experiments with the FGN sequences controlled by the Hurst exponent  $H \sim [0.3, 0.8]$ . In each set of experiments, we generated  $n = 30$  sets of sample sequences with a length of  $N = 3 \times 10^4$  via the FGN sequence generator provided by **Algorithm 1**. In order to reduce the variance of the estimation errors, we take the following arithmetic average

$$\overline{\hat{H}_{\diamond}^{\text{fgn}}} = \frac{1}{n} \sum_{i=1}^n \hat{H}_{\diamond}^{(\text{fgn}, i)}.$$

Table 3: Estimation results of Hurst exponent value for short-correlated random sequences such that  $H \sim 0.5$

$\hat{H}_{\diamond}^*$	AM	AV	GHE	HM	DFA	R/S	TTA	PM	AWC	VVL	LW	LSSD	LSV
$\mathcal{N}(0,1)$	0.4942	0.4980	0.5012	0.4994	0.4919	0.4992	0.4971	0.5067	0.4971	0.5258	0.5002	0.4977	0.4987
$\chi^2(1)$	0.4985	0.4975	0.4970	0.5234	0.4931	0.4741	0.5133	0.4992	0.5075	0.4642	0.4982	0.5001	0.4995
GE(0.25)	0.5007	0.4966	0.5003	0.5155	0.4992	0.4923	0.5101	0.5105	0.5086	0.4888	0.5003	0.5009	0.5007
$\mathcal{P}(5)$	0.4971	0.4931	0.4999	0.5020	0.4974	0.4966	0.4940	0.5019	0.4978	0.5071	0.5001	0.4999	0.5001
Exp(1)	0.4837	0.4749	0.5014	0.5128	0.5030	0.4839	0.5105	0.4784	0.4946	0.4947	0.5010	0.5024	0.5021
$\mathcal{U}(0,1)$	0.4853	0.4822	0.5002	0.4896	0.5049	0.4959	0.4987	0.4975	0.5013	0.5266	0.5001	0.5022	0.5017

For  $n = 30$  times repetitive experiments, the values of  $\overline{\hat{H}_{\diamond}^{\text{fgn}}}$  are shown in **Table 4**. The parameters  $w = 50$  and  $\text{flag} = 2$  are set the same as that for **Table 3**. Now please recall the **Figure 1** for the classification of estimation methods. In **Table 4**, it can be observed that:

- The TTA method exhibits excellent accuracy in the time-domain.
- The spectrum-domain methods are superior to the time-domain methods in general. The PM, AWC and VVL methods give similar accuracies, however the LW method is a little inferior.
- For Bayesian methods, the LSSD and LSV produce the estimations of high accuracy.
- When the sequence has long-term autocorrelation ( $H > 0.5$ ), time-domain algorithms produce underestimated values for the Hurst exponent, whereas the spectrum-domain algorithms work very well, which is consistent with the results discovered by Chen et al. [49].

Table 4: Comparison of estimation accuracy of the 13 algorithms via FGN sequences with given Hurst exponent

$\hat{H}_{\diamond}^{\text{fgn}}$	AM	AV	GHE	HM	DFA	R/S	TTA	PM	AWC	VVL	LW	LSSD	LSV
0.30	0.3023	0.2984	0.3006	0.3006	0.3078	0.3692	0.3003	0.3099	0.2919	0.3126	0.2629	0.3002	0.3003
0.35	0.3521	0.3495	0.3501	0.3500	0.3502	0.4056	0.3500	0.3614	0.3426	0.3592	0.3239	0.3496	0.3497
0.40	0.4074	0.4044	0.3994	0.3999	0.3981	0.4468	0.3988	0.4047	0.3952	0.4085	0.3844	0.4001	0.3998
0.45	0.4365	0.4353	0.4507	0.4511	0.4544	0.4856	0.4472	0.4369	0.4372	0.4402	0.4429	0.4503	0.4504
0.50	0.5000	0.4956	0.4991	0.4991	0.4995	0.5293	0.4994	0.5037	0.4989	0.4993	0.4994	0.4983	0.4985
0.55	0.5425	0.5397	0.5511	0.5512	0.5516	0.5702	0.5510	0.5561	0.5431	0.5430	0.5577	0.5521	0.5519
0.60	0.5869	0.5849	0.5999	0.6001	0.5991	0.6102	0.6017	0.5851	0.5985	0.6005	0.6127	0.6000	0.6003
0.65	0.6411	0.6394	0.6478	0.6474	0.6485	0.6539	0.6482	0.6524	0.6491	0.6432	0.6652	0.6492	0.6488
0.70	0.6679	0.6648	0.6984	0.6988	0.7057	0.6853	0.6994	0.6824	0.6955	0.6964	0.7213	0.7002	0.7000
0.75	0.7192	0.7169	0.7470	0.7472	0.7516	0.7226	0.7484	0.7459	0.7519	0.7447	0.7747	0.7496	0.7496
0.80	0.7636	0.7635	0.7948	0.7948	0.7978	0.7551	0.7990	0.7955	0.8052	0.7998	0.8288	0.7997	0.8002

## 5.4 Relative Error of Estimating Hurst Exponent

With the help of the controllable Hurst exponent  $H^{\text{fgn}}$  for the FGN sequences, we can compare the difference of various estimation methods mentioned above.

For the sequence  $\{X_j : 1 \leq j \leq N\}$  generated from the FGN sequences, suppose the estimated Hurst exponent in the  $i$ -th experiment in  $n$  repeatable experiments with estimation method  $\diamond$  is  $\hat{H}_\diamond^i$ . The relative error of estimation can be defined by

$$\eta_\diamond^i = \frac{|\hat{H}_\diamond^i - H^{\text{fgn}}|}{H^{\text{fgn}}} \times 100\%, \quad 1 \leq i \leq n \quad (110)$$

then the average relative error must be

$$\eta_\diamond = \frac{1}{n} \sum_{i=1}^n \eta_\diamond^i. \quad (111)$$

In consequence, for different estimation  $\diamond$ , we can compare their relative error to evaluate their performances with the help of (110) and (111).

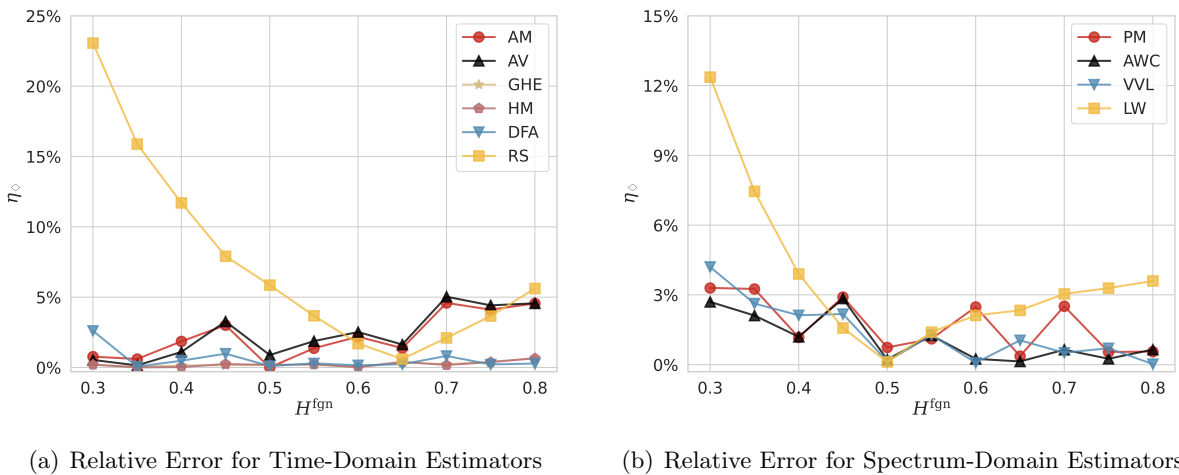


Figure 6: Comparison of Hurst Estimators via the FGN sequences with known Hurst exponent

**Figure 6** illustrates the values of  $\eta_\diamond$  in  $n = 100$  repeatable experiments with various estimation methods for the Hurst exponent of the FGN sequences. The results of the time-domain methods and the spectrum-domain methods are displayed in **Figure 6(a)** and **Figure 6(b)** respectively. Please note that the relative errors for the two Bayesian statistical methods (LSSD and LSV) and the TTA-method are not shown in the figure due to their small values (about  $1.5 \times 10^{-3}$ ).

In the **Figure 6(a)** for the time-domain methods, as the Hurst exponent value of the FGN sample sequence increases, the estimation error of most methods exhibits an upward trend. On the contrary, the relative error for the R/S method decreases with the nominal value of Hurst exponent. An interesting phenomena is that the relative error of the DFA method remains stable and its value is smaller than  $5 \times 10^{-3}$ .

In the **Figure 6(b)** for the spectrum-domain methods, all methods achieve relatively accurate estimation results. However, the error curve of the LW method exhibits a symmetric distribution around  $H = 0.5$ . To address the issue of larger errors in the lower range of  $H^{\text{fgn}}$  for the R/S method, we can improve the estimation precision by constructing the revised statistical  $\mathcal{R}_Y^{\text{AL}}$  as given in equation (71).

## 5.5 Impacts of Norm and Optimization Method on Estimation Performance

In the experiment mentioned in sub-section 5.3, we also explored the application of different linear regression methods in the estimation of the Hurst exponent. For example, in three sets of experiments

with  $H^{\text{fgn}} \in \{0.3, 0.5, 0.8\}$ , we selected the  $\ell_1$ -norm and  $\ell_2$ -norm as the optimization methods for linear regression. We fitted the parameters  $\mathbf{A}, \mathbf{b}$  obtained by each algorithm and calculated the relative errors by (110), the results as shown in Figure 7:

- Figure 7(a), Figure 7(b) and Figure 7(c) show that the average relative error  $\eta_{\diamond}$  is large than 5% just for the RS method, which does not depend on the optimization method for parameter estimation. Moreover, the estimation precision for GHE and HM methods are the same, which also does not depend on the usage of  $\ell_1$ -norm and  $\ell_2$ -norm optimization.
- Figure 7(a) shows that when  $H^{\text{fgn}}$  is small, the AWC and VVL methods are sensitive for the usage of  $\ell_1$ -norm and  $\ell_2$ -norm optimization.
- Figure 7(b) shows that when  $H^{\text{fgn}}$  is around 0.5, only the VVL method is sensitive for the usage of  $\ell_1$ -norm and  $\ell_2$ -norm optimization.
- Figure 7(c) shows that when  $H^{\text{fgn}}$  is large, only the AWC method is sensitive for the usage of  $\ell_1$ -norm and  $\ell_2$ -norm optimization.

It can be observed that most algorithms for estimating the Hurst exponent have relative estimation errors controlled at below 5% when the length of the TS is long enough. In general, the choice off  $\ell_1$ -norm and  $\ell_2$ -norm optimization is not essential for the long sequences. When the length of the TS is short, we recommend the minimum  $\ell_1$ -norm optimization for parameter estimation.

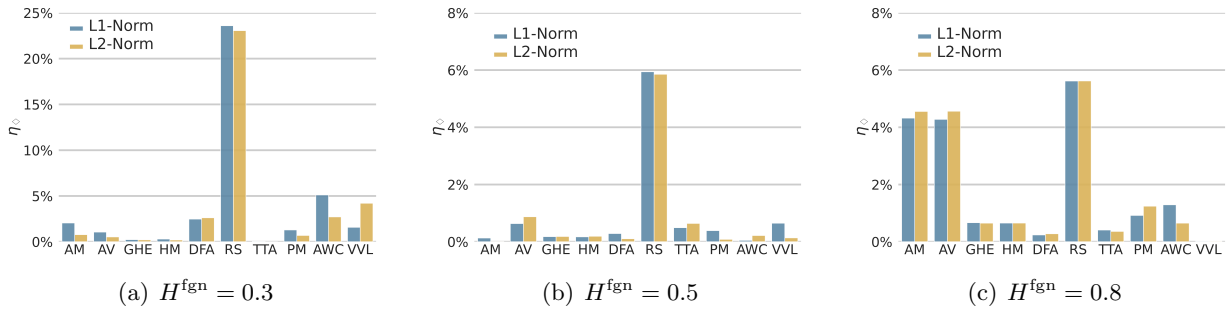


Figure 7: Relative Errors for two linear regression method

## 5.6 Hurst Exponent of Reaction Time Sequence

In the study conducted by Lauren et al. in 2021 [57], a series of speech testing experiments were designed, which included the *human-speaker* (HS) test and the *text-to-speech* (TTS) test. The *reaction time* (RT) data from 20 participants in both test groups were collected and made publicly accessible for retrieval<sup>1</sup>. In 2023, Likens applied two Bayesian methods and the DFA method to estimate the Hurst exponent of the reaction time data [13]. The results showed that all these reaction time sequences exhibited long-range memory characteristics ( $H > 0.5$ ). In this study, we also employed these data to evaluate the accuracy of the 13 methods discussed above (with a window size parameter set to  $w = 50$  and the  $\ell_2$ -norm optimization for the linear regression). The experimental results are illustrated in Figure 8.

In Figure 8, the box-body illustrates the Hurst exponent values of the reaction time sequences exhibited by 20 experimental subjects in different tests under the estimation. It is obvious that both the HS-test data set and the TTS-test data set demonstrate long-term memory characteristics in the estimated results ( $H > 0.5$ ). This experimental result aligns with the conclusion obtained by Zhang et al. [23] in 2017.

<sup>1</sup><https://royalsocietypublishing.org/doi/suppl/10.1098/rsif.2021.0272>

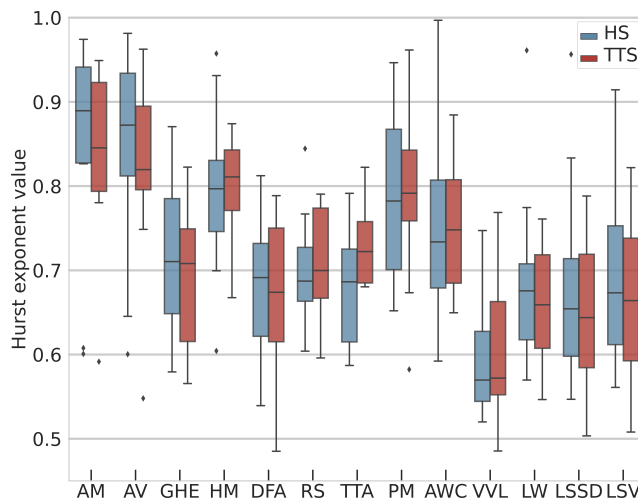


Figure 8: Estimation of reaction time sequence in HS-test and TTS-test by each method

## 5.7 Discussion

The results from subsection 5.4 indicates that the estimation accuracy of spectrum-domain methods is significantly superior to that of time-domain methods, with the two Bayesian methods demonstrating the highest precision. In terms of method selection strategy, we have the following observations:

- Time-domain methods exhibit good interpretation and no advanced programming skills are needed for implementing the estimation algorithms, whereas the implementation process of spectrum-domain methods relies on more advanced mathematical tools such as the FFT and wavelet analysis.
- With the time-domain methods, we can effectively demonstrate the correspondence between partial statistical properties of sequences and sample scales (typically represented by a straight line). This is also why time-domain methods are highly popular and widely applied.
- The Bayesian methods provides good accuracy, but the optimization algorithms or fixed-point algorithms are necessary.

In addition to the 13 estimation methods mentioned above, there are other methods not mentioned in this paper. For example, the *maximum likelihood estimation* (MLE) method for estimating the Hurst exponent is known for its implementation difficulty and high time complexity. For the interested readers, please refer to the references [58–60].

In 2022, Gómez et al. proposed the *Kolmogorov-Smirnov* (KS) method based on the GHE method and TTA method [61]. The KS method estimates the Hurst exponent by calculating the Kolmogorov-Smirnov (KS) statistic distance between the empirical distributions of samples [62]. Gomez et al. [61] provided the Python code for the KS method and it is omitted here.

In our experiment, it has been observed that for certain shorter time sequences [24], most estimation methods fail to produce accurate results. However, there exist a few methods that have good estimation performance, such as the GHE method, LW method, and LSVmethod. As for other time-domain methods, such as the R/S method, we can take the linear interpolation technique and use interpolation points to construct the sample sequences of lengths  $\{N/2, N/4, \dots\}$ . This approach extends the applicability of the estimation methods for the Hurst exponent to the shorter time sequences.

It should remarked that there are also possible ways for estimating the Hurst exponent via the new techniques for analyzing the time sequences with LTM. For the time-domain algorithms, the TTA method has demonstrated its commendable performance. The topological structures of the time sequences [63–65] are attracting more and more researchers to discover more intrinsic characteristics. For the frequency-domain methods, the two wavelet-based approaches, viz. AWC and VVL, have demonstrated novel perspectives for us. The mode decomposition of time series [66, 67] is a new

interesting point of current researches, and this may potentially lead to the development of additional computational methods in the frequency-domain.

## 6 Conclusions

In this paper, we summarized 13 typical methods for estimating the Hurst exponent and categorized them into different classes based on different strategies:

- time-domain methods and spectrum-domain methods based on the representation of time sequence;
- linear regression methods and Bayesian methods based on the parameter estimation method.

Both the mathematical principle and algorithmic pseudo-codes are provided for these 13 methods, which helps the researchers and potential users to implement these methods with concrete programming language based on a unified framework.

Our contributions are summarized as follows:

- A general sequence partition framework was proposed for various time-domain methods based on the optimal approximate length and feasible sequence grouping approach.
- The fixed-point algorithm, local minimum search algorithm, and linear regression method based on  $\ell_1$ -norm are applied to improve the accuracy of estimating the Hurst exponent with available estimation methods.
- The estimation methods are classified with two perspectives, viz. the sequence representation and parameter estimation.
- The sequences generated via FGN and pure random sequences are used to design a series of experiments to test the accuracy of the 13 estimators discussed above.
- The flowcharts of R/S method and DFA method are provided for helping the readers to understand the essence and steps of the algorithms concerned.

The numerical experiments and error analysis for the 13 estimation methods shows that:

- The estimation accuracy of spectrum-domain methods is superior to time-domain methods, with a relative error of less than 6% in general.
- When the value of Hurst exponent is small (say  $H < 0.35$ ), the relative errors of the estimation obtained by the R/S method and LW method are significantly larger than 5%;
- The choice of  $\ell_1$ -norm and  $\ell_2$ -norm has little impact on the estimation accuracy.
- The estimation with the practical data captured from the human behavioral experiment available online implies that each estimation method can effectively reveal the long-term memory features of the sequences, which confirming the suitability of the 13 methods.

For the off-line applications where the Hurst exponent is involved, we recommend the TTA method for the time-domain methods, the LSSD and LSV for the Bayesian methods, and the PM method for the spectrum-domain methods. For the real-time applications in which the Hurst exponent should be estimated dynamically, we recommend the R/S method to reduce the computational complexity since both the range and standard deviation can be estimated iteratively with the time clock.

## Acknowledgments

This work was supported in part by the National Natural Science Foundation of China under grant number 62167003, in part by Hainan Provincial Natural Science Foundation of China under grant numbers 720RC616 and 623RC480, in part by the Research Project on Education and Teaching Reform in Higher Education System of Hainan Province under grant number Hnjg2023ZD-26, in part by the Specific Research Fund of The Innovation Platform for Academicians of Hainan Province, and in part by the Hainan Province Key R & D Program Project under grant number ZDYF2021GXJS010.

## A Algorithm for Local Minimization on Interval $[a, b]$

The algorithm for finding a local minimum of a function of a single variable is as follows:

---

**Algorithm 24** A local minimum of real valued function, say  $\phi : [a, b] \times \dots \rightarrow \mathbb{R}, (x, \dots) \mapsto y$ .

---

**Input:** Function  $\phi$ ; Interval  $[a, b]$ , precision  $\epsilon$ , extra parameters  $\langle \dots \rangle$ .

**Output:** A local minimum for  $\phi$  in  $[a, b]$ .

```

1: procedure LOCMINSOLVER( $\phi, [a, b], \epsilon, \langle \dots \rangle$ )
2:    $c \leftarrow (3 - \sqrt{5})/2; d \leftarrow 0; e \leftarrow 0;$ 
3:    $v, w, x \leftarrow a + c \cdot (b - a);$ 
4:    $f_v, f_w, f_x \leftarrow \phi(x, \langle \dots \rangle);$ 
5:   while True do
6:      $m \leftarrow (a + b)/2;$ 
7:      $t_1 \leftarrow \epsilon^2 \cdot |x| + \epsilon/3;$ 
8:     if  $|x - m| \leq t_1^2 - (b - a)/2$  then
9:       break;
10:    end if
11:    if  $|e| > t_1$  then
12:       $r \leftarrow (x - w) \cdot (f_x - f_v);$ 
13:       $q \leftarrow (x - v) \cdot (f_x - f_w);$ 
14:       $p \leftarrow (x - v) \cdot q - (x - w) \cdot r;$ 
15:       $q \leftarrow 2(q - r);$ 
16:      if  $q > 0$  then
17:         $p \leftarrow -p;$ 
18:      else
19:         $q \leftarrow -q;$ 
20:      end if
21:       $r \leftarrow e; e \leftarrow d;$ 
22:    end if
23:    if  $|p| \geq \frac{|qr|}{2} \vee p \leq q(a - x) \vee p \geq q(b - x)$  then
24:      if  $x \leq m$  then
25:         $e \leftarrow b - x;$ 
26:      else
27:         $e \leftarrow a - x;$ 
28:      end if
29:       $d \leftarrow c \cdot e;$ 
30:    else
31:       $d \leftarrow p/q; u \leftarrow x + d;$ 
32:      if  $(u - a) < t_1^2 \vee (b - u) < t_1^2$  then
33:        if  $x < m$  then
34:           $d \leftarrow t_1;$ 
35:        else
36:           $d \leftarrow -t_1;$ 
37:        end if
38:      end if
39:    end if
40:    if  $|d| \geq t_1$  then
41:       $u \leftarrow x + d;$ 
42:    else if  $d > 0$  then
43:       $u \leftarrow x + t_1;$ 

```

```

44:     else
45:          $u \leftarrow x - t_1$ ;
46:     end if
47:      $f_u \leftarrow \phi(u, \langle \cdot \cdot \cdot \rangle)$ ;
48:     if  $f_u \leq f_x$  then
49:         if  $u < x$  then
50:              $b \leftarrow x$ ;
51:         else
52:              $a \leftarrow x$ ;
53:         end if
54:          $v \leftarrow w$ ;  $f_v \leftarrow f_w$ ;  $w \leftarrow x$ ;  $f_w \leftarrow f_x$ ;
55:          $x \leftarrow u$ ;  $f_x \leftarrow f_u$ ;
56:     else
57:         if  $u < x$  then
58:              $a \leftarrow u$ ;
59:         else
60:              $b \leftarrow u$ ;
61:         end if
62:         if  $f_u \leq f_w \vee w = x$  then
63:              $v \leftarrow w$ ;  $f_v \leftarrow f_w$ ;  $w \leftarrow u$ ;  $f_w \leftarrow f_u$ ;
64:         else if  $f_u \leq f_v \vee v = x \vee v = w$  then
65:              $v \leftarrow u$ ;  $f_v \leftarrow f_u$ ;
66:         end if
67:     end if
68: end while
69: return  $x$ ;
70: end procedure

```

---

## Code Availability

The code for the implementations of the algorithms discussed in this paper can be downloaded from the following GitHub website

<https://github.com/GrAbsRD/HurstExponent>

For the convenience of easy usage, both Python and Octave/MATLAB codes are provided.

## Data Availability

The data set supporting the results of this study is available on the GitHub website

<https://github.com/ZhiQiangFeng/HurstExponentTestData>

The repository includes a README file with essential information on data access and use. For any questions regarding the data, please contact the author with the e-mail: [z.q.feng@foxmail.com](mailto:z.q.feng@foxmail.com).

## References

- [1] H. E. Hurst. Long-term storage capacity of reservoirs. *Transactions of the American Society of Civil Engineers*, 116(1):770–799, 1951.
- [2] H. E. Hurst, R.P. Black, and Y. M. Simaika. *Long-term Storage: An Experimental Study*. Constable, 1965.

- [3] H. E. Hurst. Methods of using long-term storage in reservoirs. *Proceedings of the institution of Civil Engineers*, 5(5):519–543, 1956.
- [4] J. Beran. *Statistics for long-memory processes*. Number 61 in Monographs on statistics and applied probability. Chapman & Hall.
- [5] M. S. Taqqu, V. Teverovsky, and W. Willinger. Estimators for Long-Range Dependence: An Empirical Study. *Fractals*, 3(04):785–798, 1995.
- [6] A.-L. Barabási and T. Vicsek. Multifractality of self-affine fractals. *Physical Review A*, 44(4):2730, 1991.
- [7] T. Higuchi. Approach to an irregular time series on the basis of the fractal theory. *Physica D: Nonlinear Phenomena*, 31(2):277–283, 1988.
- [8] C.-K. Peng, S. V. Buldyrev, S. Havlin, M. Simons, H. E. Stanley, and A. L. Goldberger. Mosaic organization of DNA nucleotides. *Physical Review E*, 49:1685–1689, Feb 1994.
- [9] H. Lotfalinezhad and A. Maleki. TTA, a new approach to estimate Hurst exponent with less estimation error and computational time. *Physica A: Statistical Mechanics and its Applications*, 553:124093, 2020.
- [10] A. Gómez-Águila and M. A. Sánchez-Granero. A theoretical framework for the TTA algorithm. *Physica A: Statistical Mechanics and its Applications*, 582:126288, 2021.
- [11] H. Tyralis and D. Koutsoyiannis. Simultaneous estimation of the parameters of the Hurst-Kolmogorov stochastic process. *Stochastic Environmental Research and Risk Assessment*, 25:21–33, 2011.
- [12] D. Koutsoyiannis. Climate change, the Hurst phenomenon, and hydrological statistics. *Hydrological Sciences Journal*, 48(1):3–24, 2003.
- [13] A. D. Likens, M. Mangalam, A. Y. Wong, A. C. Charles, and C. Mills. Better than DFA? A Bayesian Method for Estimating the Hurst Exponent in Behavioral Sciences. arXiv:2301.1126.
- [14] J. R. M. Hosking. Fractional Differencing. *Biometrika*, 68(1):165–176, 04 1981.
- [15] J. Geweke and S. Porter-Hudak. The estimation and application of long memory time series models. *Journal of time series analysis*, 4(4):221–238, 1983.
- [16] H. Künsch. *Statistical aspects of self-similar processes*, pages 67–74. De Gruyter, Berlin, Boston, 1987.
- [17] P. M. Robinson. Gaussian Semiparametric Estimation of Long Range Dependence. *The Annals of Statistics*, 23(5):1630 – 1661, 1995.
- [18] P. C. B. Phillips and K. Shimotsu. Local Whittle Estimation in Nonstationary and Unit Root Cases. *The Annals of Statistics*, 32(2), Apr 2004.
- [19] P. Flandria. On the Spectrum of Fractional Brownian Motions. *IEEE Transactions on Information Theory*, 35(1):197–199, 1989.
- [20] P. Flandrin. Wavelet Analysis and Synthesis of Fractional Brownian Motion. *IEEE Transactions on Information Theory*, 38(2):910–917, 1992.
- [21] I. Simonsen, A. Hansen, and O. M. Nes. Determination of the Hurst Exponent by Use of Wavelet Transforms. *Physical Review E*, 58(3):2779, 1998.
- [22] I. Simonsen. Measuring Anti-Correlations in the Nordic Electricity Spot Market by Wavelets. *Physica A: Statistical Mechanics and its applications*, 322:597–606, 2003.

- [23] H.-Y. Zhang, M.-C. Kang, J.-Q. Li, and H.-T. Liu. R/S analysis of reaction time in Neuron Type Test for human activity in civil aviation. *Physica A: Statistical Mechanics and its Applications*, 469:859–870, 2017.
- [24] J.-Q. Li, H.-Y. Zhang, Y. Zhang, and H.-T. Liu. Systematic assessment of intrinsic factors influencing visual attention performances in air traffic control via clustering algorithm and statistical inference. *Plos One*, 13(10):e0205334, 2018.
- [25] L. Moundjian, P.-J. Maes, S. D. Bella, L. M. Decker, B. Moens, P. Feys, and M. Leman. De-trended fluctuation analysis of gait dynamics when entraining to music and metronomes at different tempi in persons with multiple sclerosis. *Scientific Reports*, 10(1):12934, 2020.
- [26] H. L. Shang. A Comparison of Hurst Exponent Estimators in Long-Range Dependent Curve Time Series. *Journal of Time Series Econometrics*, 12(1), 2020.
- [27] A. H. Hamza and M. Y. Hmood. Comparison of Hurst exponent estimation methods. *Journal of Economics and Administrative Sciences*, 27(128), 2021.
- [28] S. Lahmiri. A nonlinear analysis of cardiovascular diseases using multi-scale analysis and generalized hurst exponent. *Healthcare Analytics*, 3:100142, 2023.
- [29] R. Paul, V. Parameswaran, and S. Basu. Morphology of fracture profiles and toughness: competition between inter and transgranular fracture in two dimensional brittle solids. preprint, available at Research Square, 2024.
- [30] B. B. Mandelbrot and J. R. Wallis. Noah, Joseph, and Operational hydrology. *Water resources research*, 4(5):909–918, 1968.
- [31] B. B. Mandelbrot and J. R. Wallis. Robustness of the Rescaled Range R/S in the Measurement of Noncyclic Long Run Statistical Dependence. *Water resources research*, 5(5):967–988, 1969.
- [32] B. B. Mandelbrot. *The Fractal Geometry of Nature*. Echo Point Books, San Francisco, 1982.
- [33] A. V. Oppenheim and R. W. Schaffer. *Discrete-Time Signal Processing*. Prentice Hall, 3rd edition, 2010.
- [34] J. Cooley and J. Tukey. An algorithm for the machine calculation of complex Fourier series. *Mathematical Computation*, 19(90):297–301, 1965.
- [35] M. Begum, J. Ferdush, and M. S. Uddin. A Hybrid robust watermarking system based on discrete cosine transform, discrete wavelet transform, and singular value decomposition. *Journal of King Saud University - Computer and Information Sciences*, 34(8, Part B):5856–5867, 2022.
- [36] N. Kehtarnavaz. *Digital Signal Processing System Design*. Academic Press, Burlington, 2nd edition, 2008. Chapter 7: Frequency Domain Processing, pages: 175–196.
- [37] A. Haar. *Zur Theorie der orthogonalen Funktionensysteme*. Georg-August-Universitat, Göttingen., 1909.
- [38] I. Daubechies. *Ten Lectures on Wavelets*. SIAM, 1992.
- [39] D. Delignieres, K. Torre, and P. Bernard. Transition from Persistent to Anti-Persistent Correlations in Postural Sway Indicates Velocity-Based Control. *PLoS Computational Biology*, 7:e1001089, 02 2011.
- [40] B. B. Mandelbrot and J. W. V. Ness. Fractional Brownian Motions, Fractional Noises and Applications. *SIAM review*, 10(4):422–437, 1968.
- [41] R. B. Davies and D. S. Harte. Tests for Hurst effect. *Biometrika*, 74(1):95–101, 1987.
- [42] X.-D. Zhang. *Matrix Analysis and Applications*. Cambridge University Press, 2017.

- [43] C. C. Paige and Z. Strakos. Scaled total least squares fundamentals. *Numerische Mathematik*, 91(1):117–146, 2002.
- [44] H.-Y. Zhang and Z. Geng. Novel Interpretation for Levenberg-Marquardt algorithm. *Computer Engineering and Applications*, 45(19):5–8, 2009.
- [45] H.-Y. Zhang. *Multi-View Image-Based 2D and 3D Scene Modeling: Principles and Applications of Manifold Modeling and Cayley Methods*. Science Press, Beijing, 2022.
- [46] Z.-Q. Feng and H.-Y. Zhang. A Novel Approach for Estimating Parameters of Multivariate Linear Model via Minimizing  $\ell_1$ -Norm of Residual Vector and Basis Pursuit. *Journal of Hainan Normal University (Natural Science)*, 35(3):11, 2022.
- [47] H.-Y. Zhang, W. S., X. Chen, R.-J. Lin, and Y. Zhou. Fixed-point algorithms for solving the critical value and upper tail quantile of Kuiper’s statistics. *Heliyon*, 10(7):e28274, 2024.
- [48] R. P. Brent. *Algorithms for minimization without derivatives*. Courier Corporation, 2013.
- [49] J. Chen, X.-H. Tan, and Z. Jia. Performance analysis of seven estimation algorithms about the Hurst coefficient. *Computer Applications*, 26(4):945–947, 2006.
- [50] T. Di Matteo, T. Aste, and M. M. Dacorogna. Scaling behaviors in differently developed markets. *Physica A: Statistical Mechanics and its Applications*, 324(1-2):183–188, 2003.
- [51] C.-K. Peng, S. V. Buldyrev, S. Havlin, M. Simons, H. E. Stanley, and A. L. Goldberger. Mosaic organization of DNA nucleotides. *Physical Review E*, 49(2):1685, 1994.
- [52] R. Weron. Estimating long-range dependence: finite sample properties and confidence intervals. *Physica A: Statistical Mechanics and its Applications*, 312(1):285–299, 2002.
- [53] A. A. Annis and E. H. Lloyd. The expected value of the adjusted rescaled Hurst range of independent normal summands. *Biometrika*, 63(1):111–116, 1976.
- [54] E. E. Peters. *Fractal Market Analysis: Applying Chaos Theory to Investment and Economics*, volume 24. John Wiley & Sons, 1994.
- [55] P. Abry and D. Veitch. Wavelet Analysis of Long-Range-Dependent Traffic. *IEEE Transactions on Information Theory*, 44(1):2–15, 1998.
- [56] D. Koutsoyiannis. Internal report: <http://www.itia.ntua.gr/getfile/537/2/2003HSJHurstSuppl.pdf>.
- [57] L. Bloomfield, E. Lane, M. Mangalam, and D. G. Kelty-Stephen. Perceiving and remembering speech depend on multifractal nonlinearity in movements producing and exploring speech. *Journal of The Royal Society Interface*, 18(181):20210272, 2021.
- [58] A. Guerrero and L. A. Smith. A maximum likelihood estimator for long-range persistence. *Physica A: Statistical Mechanics and its Applications*, 355(2-4):619–632, 2005.
- [59] Y.-C. Chang. Efficiently Implementing the Maximum Likelihood Estimator for Hurst Exponent. *Mathematical Problems in Engineering*, 2014, 2014.
- [60] M. Garcin. A comparison of maximum likelihood and absolute moments for the estimation of Hurst exponents in a stationary framework. *Communications in nonlinear science and numerical simulation*, 114:106610, 2022.
- [61] A. Gómez-Águila, J. E. Trinidad-Segovia, and M. A. Sánchez-Granero. Improvement in Hurst exponent estimation and its application to financial markets. *Financial Innovation*, 8(1):1–21, 2022.

- [62] J. L. Hodges Jr. The significance probability of the Smirnov two-sample test. *Arkiv för matematik*, 3(5):469–486, 1958.
- [63] M. Gidea and Y. Katz. Topological data analysis of financial time series: Landscapes of crashes. *Physica A: Statistical Mechanics and its Applications*, 491:820–834, 2018.
- [64] A. Karan and A. Kaygun. Time series classification via topological data analysis. *Expert Systems with Applications*, 183:115326, 2021.
- [65] A. B. El-Yaagoubi, M. K. Chung, and H. Ombao. Topological data analysis for multivariate time series data. *Entropy*, 25(11), 2023.
- [66] J. Gao and S.-J. Peng. Analysis of complex time series based on emd energy entropy plane. *Nonlinear Dynamics*, 96:465–482, 2019. <https://doi.org/10.1007/s11071-019-04800-5>.
- [67] H.-Y. Pan, Y. Yang, X. Li, J.-D. Zheng, and J.-S. Cheng. Symplectic geometry mode decomposition and its application to rotating machinery compound fault diagnosis. *Mechanical Systems and Signal Processing*, 114:189–211, 2019.